

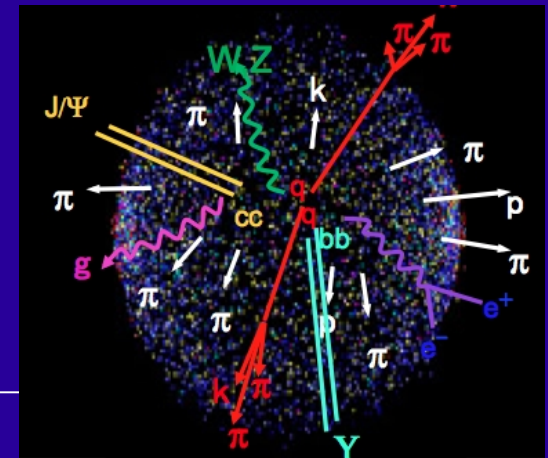
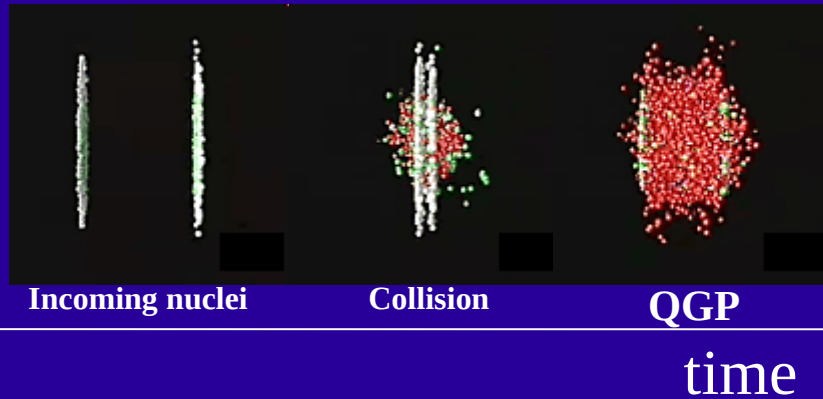
Run 2 Results on Heavy Ions from ATLAS Experiment



Helena Santos,
LIP, FCUL



Heavy Ion Collisions



Final states providing insight into the QGP:

Global observables

Particle correlations - initial conditions, geometry, collective behaviour

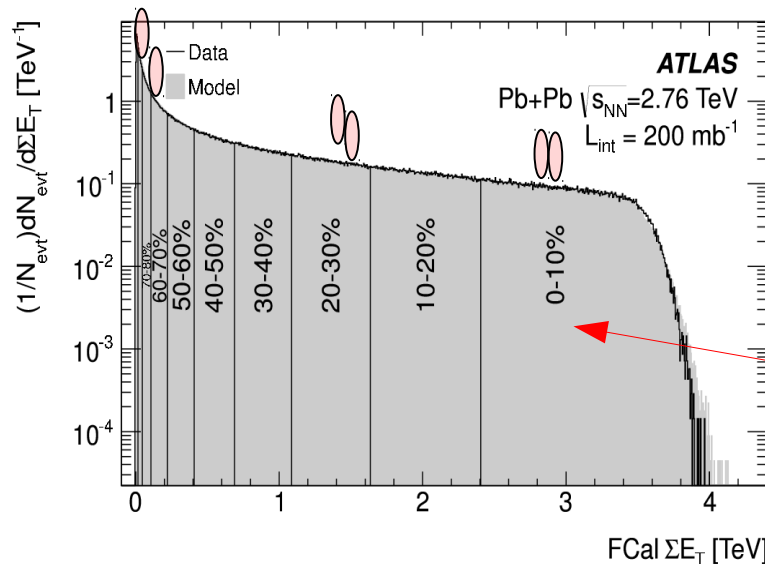
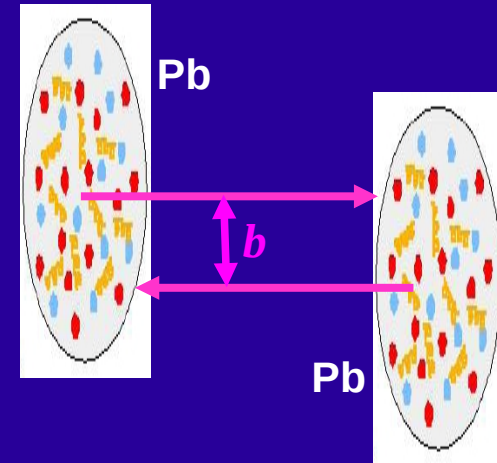
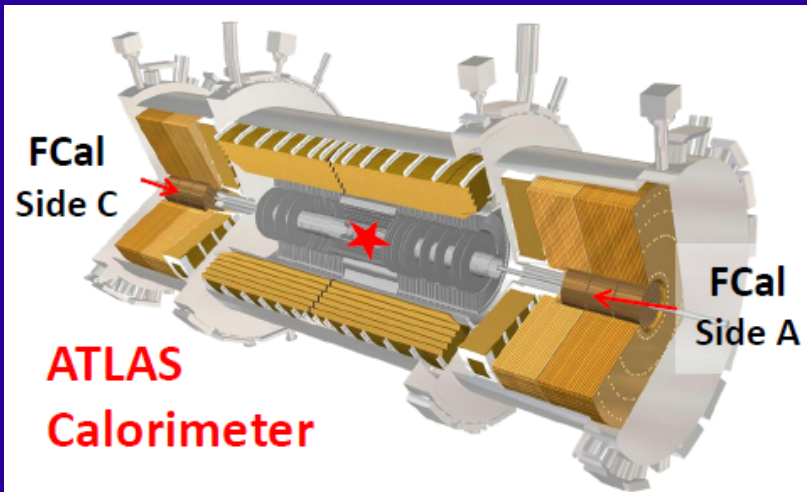
Hard probes

Colorless objects: electroweak bosons – reference, nPDFs

Colored objects: hadrons, jets, quarkonia – Debye screening, partonic energy loss

Collisions Centrality

HI collision's dynamics controlled by impact parameter " b "



Transverse energy, E_T , deposited in Forward Calorimeter.

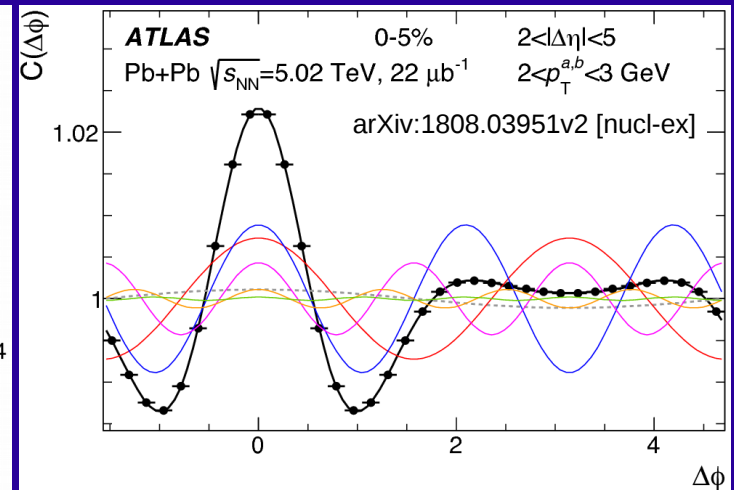
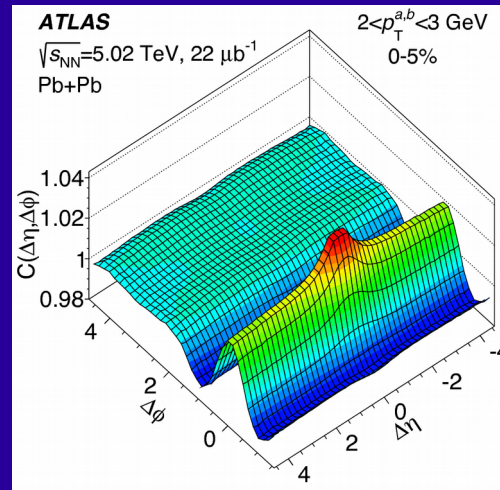
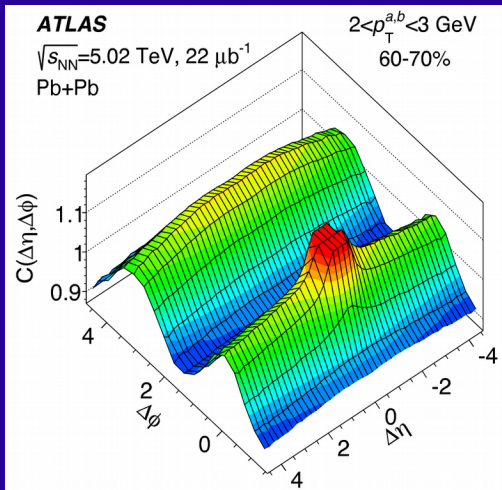
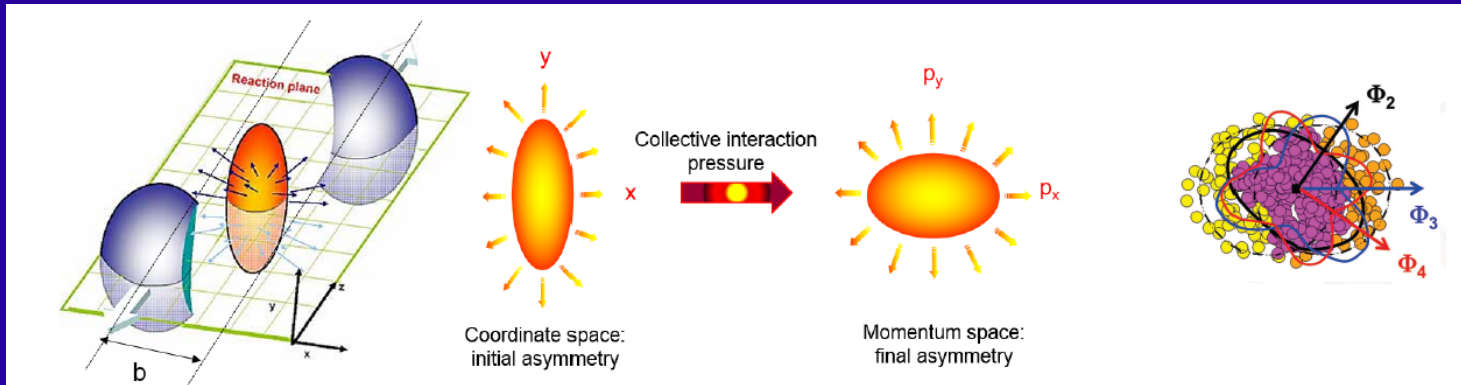
The nuclear thickness function, T_{AA} , and number of participants in a collision, N_{part} , for each centrality interval is estimated using the Glauber model.

Flow

Anisotropic spatial collective motion is described by a Fourier expansion of particle distribution in azimuthal angle ϕ

$$\frac{dN}{d\phi} \propto 1 + 2 \sum_{n=1}^{\infty} v_n \cos n(\phi - \Phi_n)$$

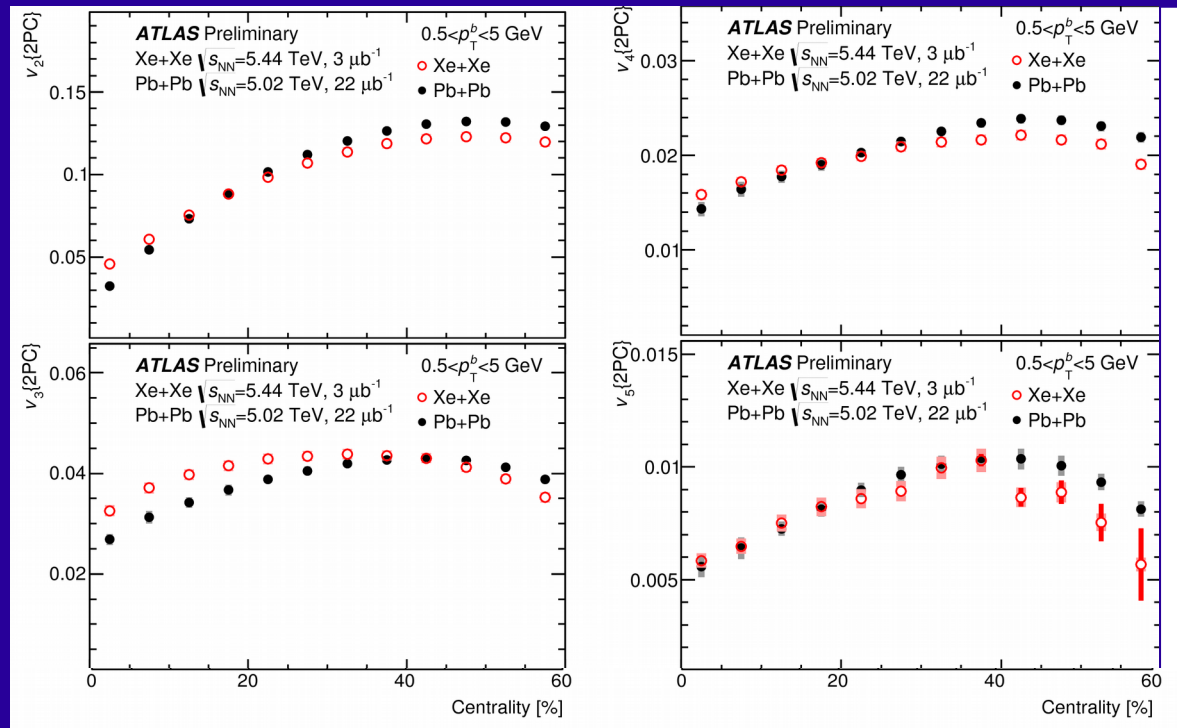
High order coefficients are associated with fluctuations of nucleon positions in the overlap



$v_n\{2PC\}$ in **Xe+Xe** and **Pb+Pb** collisions

ATLAS-CONF-2018-011

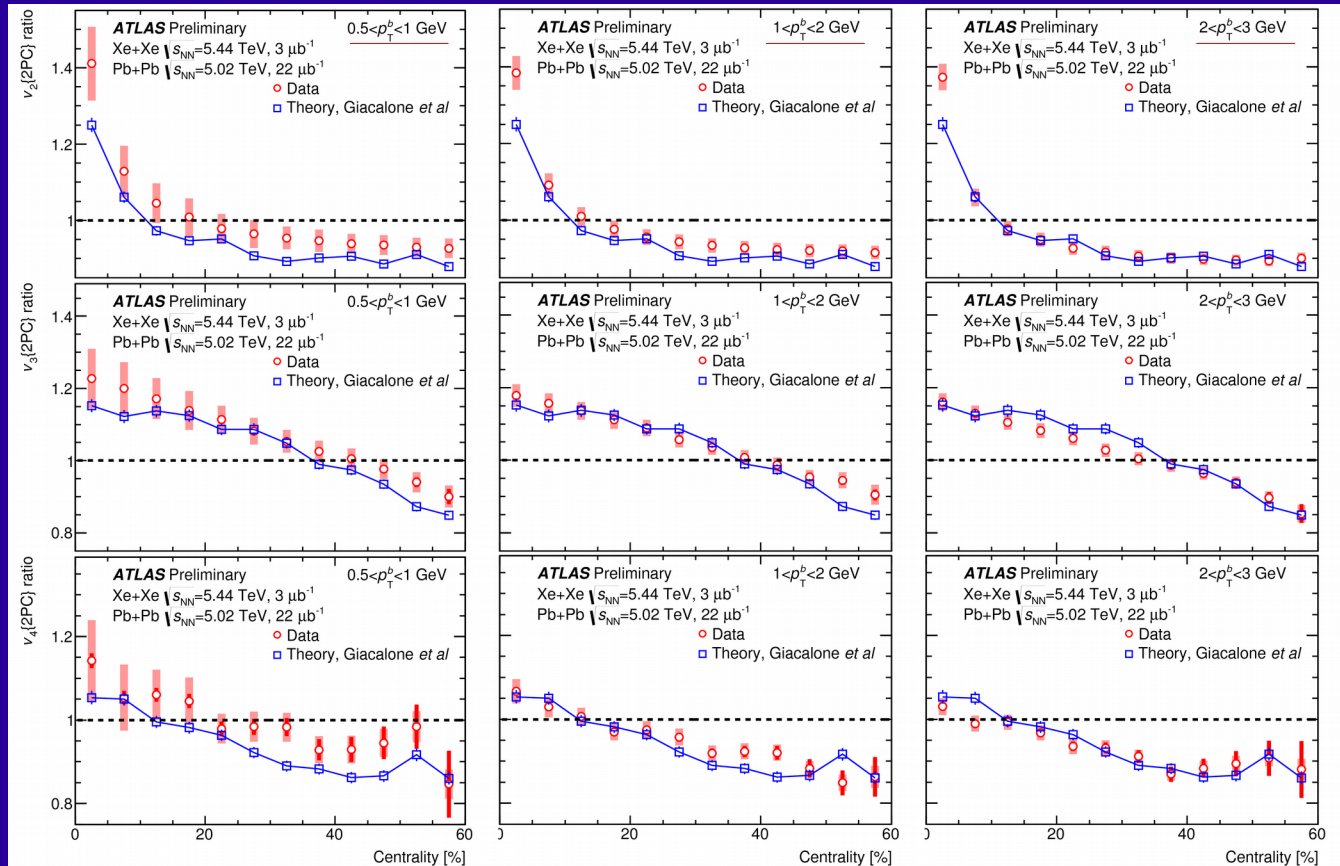
Xe is smaller → larger EbyE fluctuations → larger eccentricities
than Pb → larger viscous effects (1711.08499)



- v_n increases from central to peripheral collisions, peaking around 30–40% centrality.
- v_2 and v_3 are clearly larger in central Xe+Xe collisions.

v_n in Xe+Xe and Pb+Pb collisions - ratios

ATLAS-CONF-2018-011



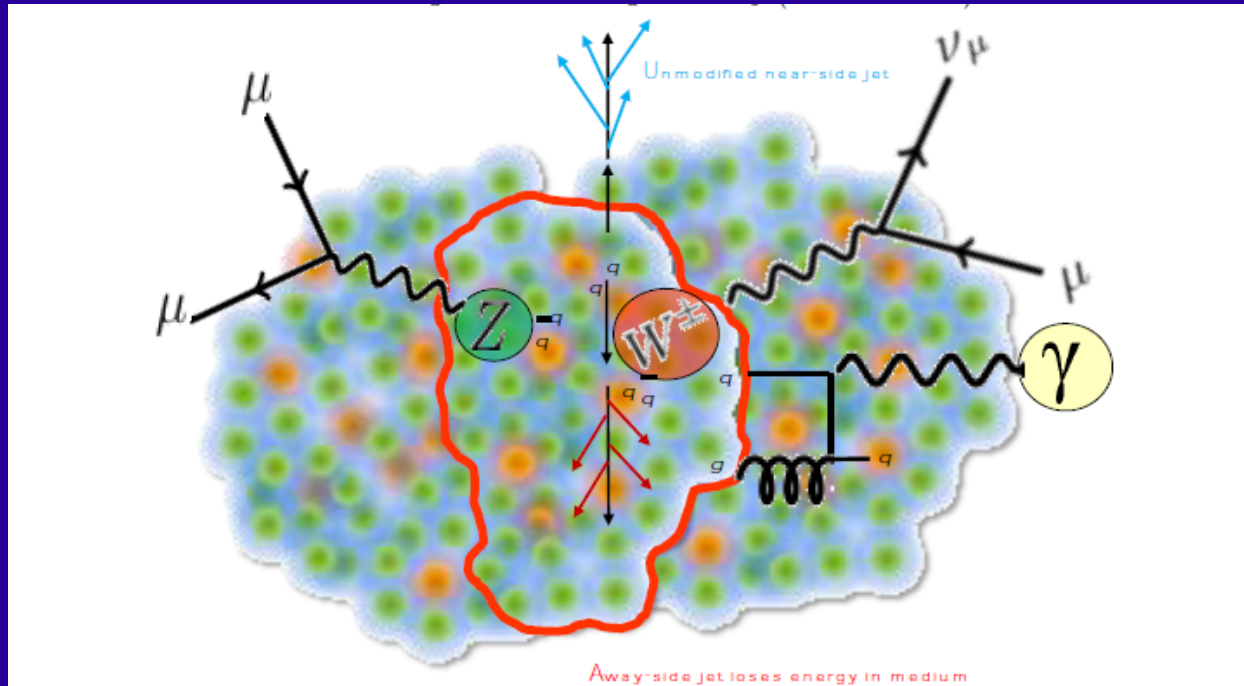
- Ratios have weak dependence in p_T^b . ($0.5 < p_T^a < 5.0$ GeV)
- Ratios for v_2 decrease with decreasing centrality becoming smaller than unity by 10–15% centrality.
- For v_3 the Xe+Xe values are larger than Pb+Pb over 0–30% centrality.
- Hydrodynamic predictions (1711.08499) describe data well.

Messages from flow

- Significant harmonic (v_2 - v_5) observed in Pb+Pb collisions reflecting the nuclear overlap and fluctuations of the initial nucleon-nucleon positions.
- The long range “ridge” and “cone” structures in two-particle correlation function at low p_T can be explained by flow effects.
- Hydrodynamics (also) describes flow in Xe+Xe collisions.

Electroweak probes

W/Z, photons, are not supposed to interact with QGP.



Can be used as benchmarks for in-medium effects.

Can also be used to check models of collision geometry (Glauber). Their production is expected to scale with number of nucleon-nucleon collisions.

Systematic study of partonic energy loss in Z and photon associated to jets.

$$R_{AA} = \frac{N_{AA}}{\langle T_{AA} \rangle \times \sigma_{pp}}$$

Yields in Pb+Pb collisions, (in medium)

Nuclear thickness function $\langle N_{\text{coll}} \rangle / \sigma_{\text{NN}}$

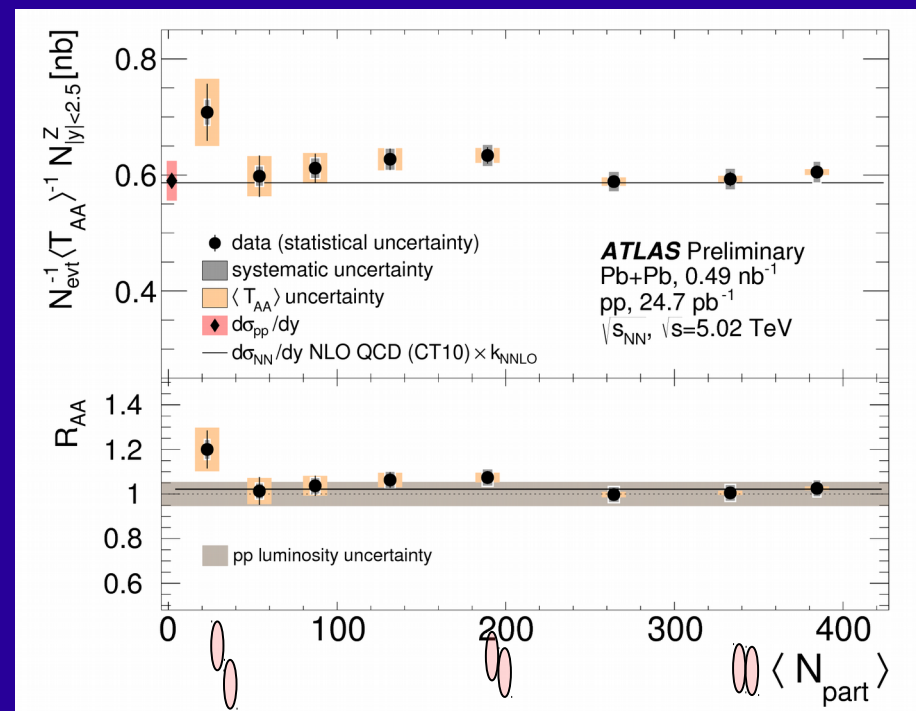
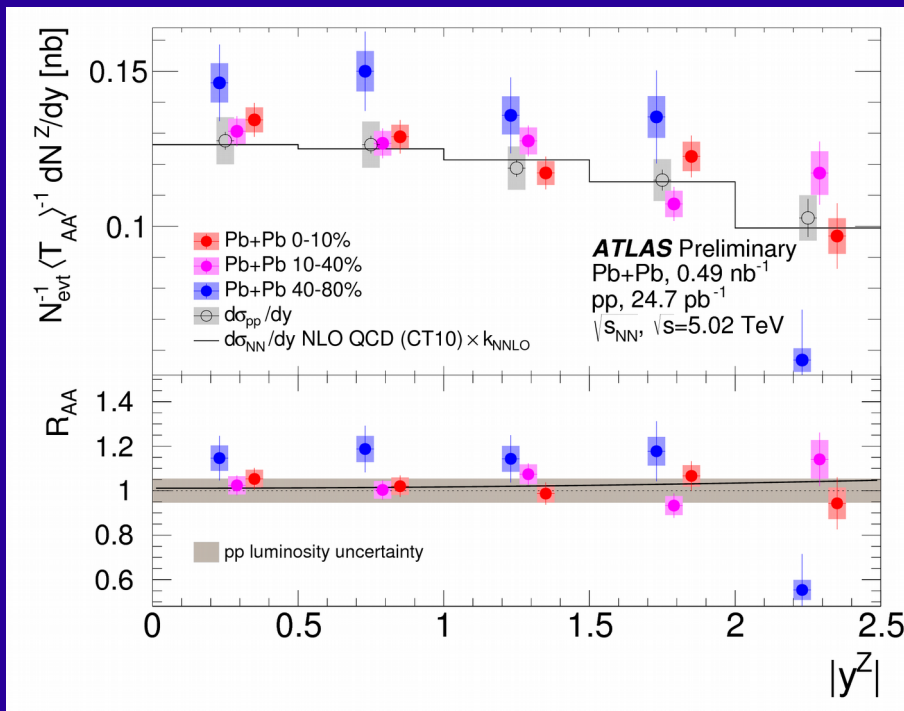
Cross section in pp collisions (in vacuum)

- Nuclear modification factor quantifies the change of yields, relatively to the production in vacuum.
- Any deviation from unity points to suppression or enhancement of yields.

Electroweak probes in Pb+Pb collisions – Z^0

10

ATLAS-CONF-2017-010

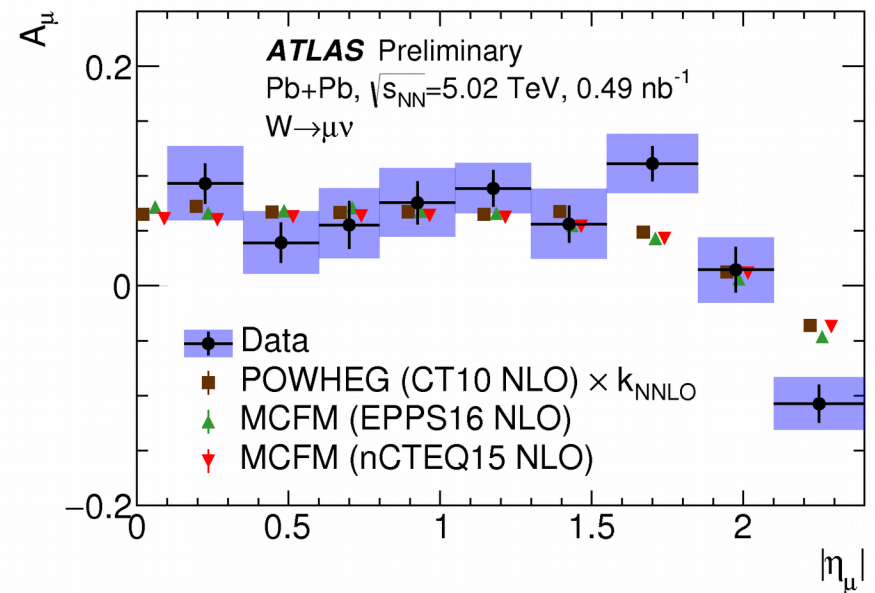
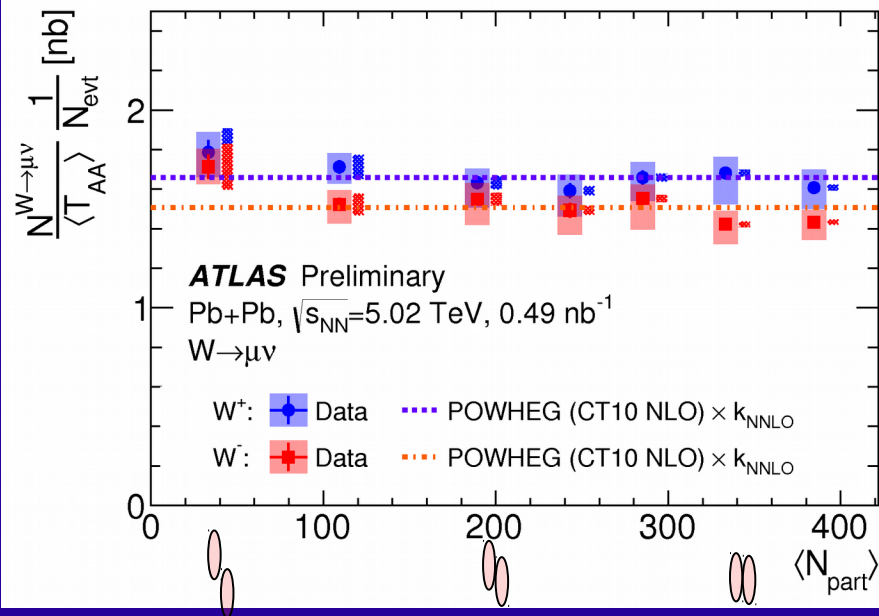


- R_{AA}^Z is expected to be greater than unity by about 2.5% due to isospin effect.
- Consistent with unity within uncertainties. Excess in the most peripheral bin?

Electroweak probes in Pb+Pb collisions - W^\pm 11

ATLAS-CONF-2017-067

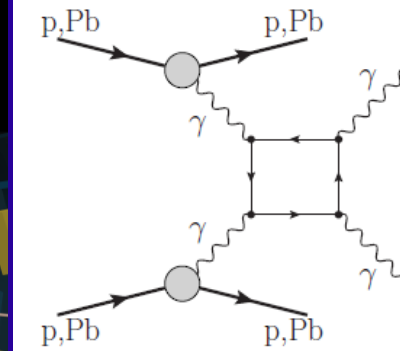
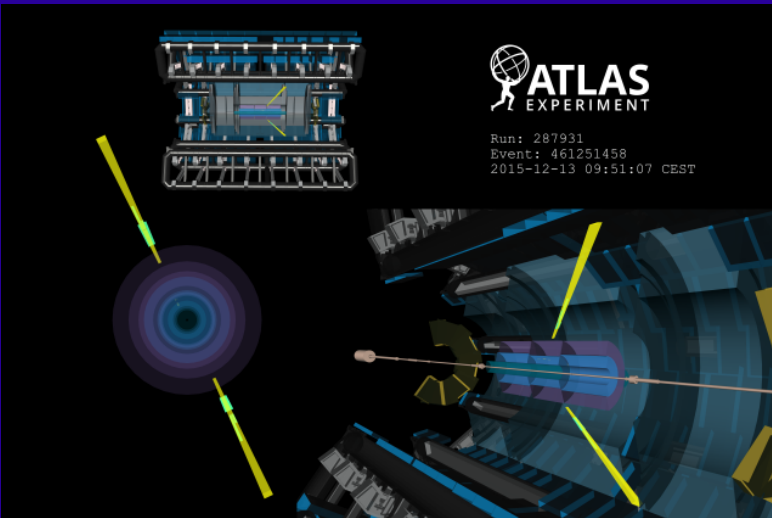
$$A_\ell(\eta_\ell) = \frac{dN_{W^+ \rightarrow \ell^+ \nu} / d\eta_\ell - dN_{W^- \rightarrow \ell^- \bar{\nu}} / d\eta_\ell}{dN_{W^+ \rightarrow \ell^+ \nu} / d\eta_\ell + dN_{W^- \rightarrow \ell^- \bar{\nu}} / d\eta_\ell}$$



- Yields of W bosons divided by T_{AA} are independent of centrality.
- $W^+ \rightarrow \mu^+ \nu$ yields are systematically $\sim 10\%$ larger than $W^- \rightarrow \mu^- \bar{\nu}$ yields.
- Good agreement with predictions, both that ascribe free-nucleon PDF and nPDF, for $|\eta_\mu| < 1.4$. Three sigma at forward.

Electroweak probes - LbyL

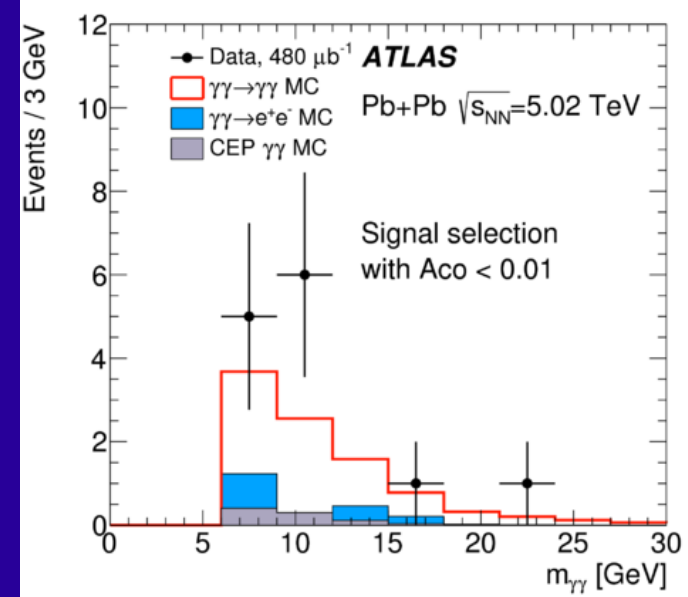
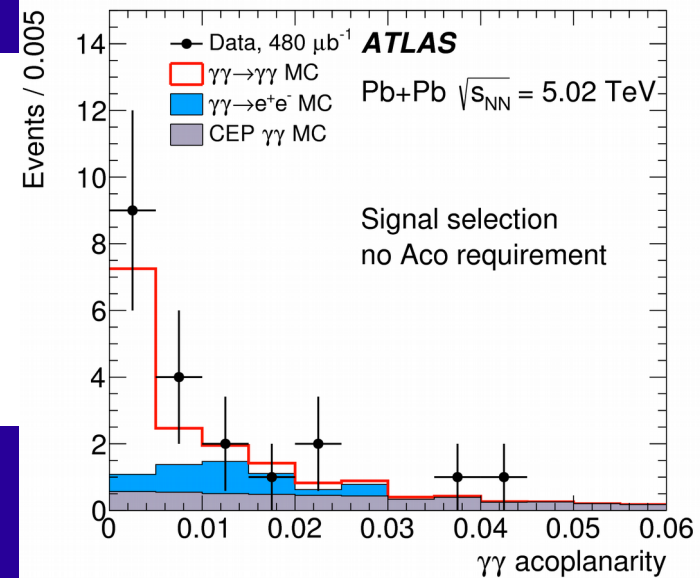
12



Evidence of LbyL scattering: 4.4 (3.8) σ

$\sigma_{\text{fid}} = 70 \pm 24$ (stat) ± 17 (syst) nb, in agreement with SM predictions.

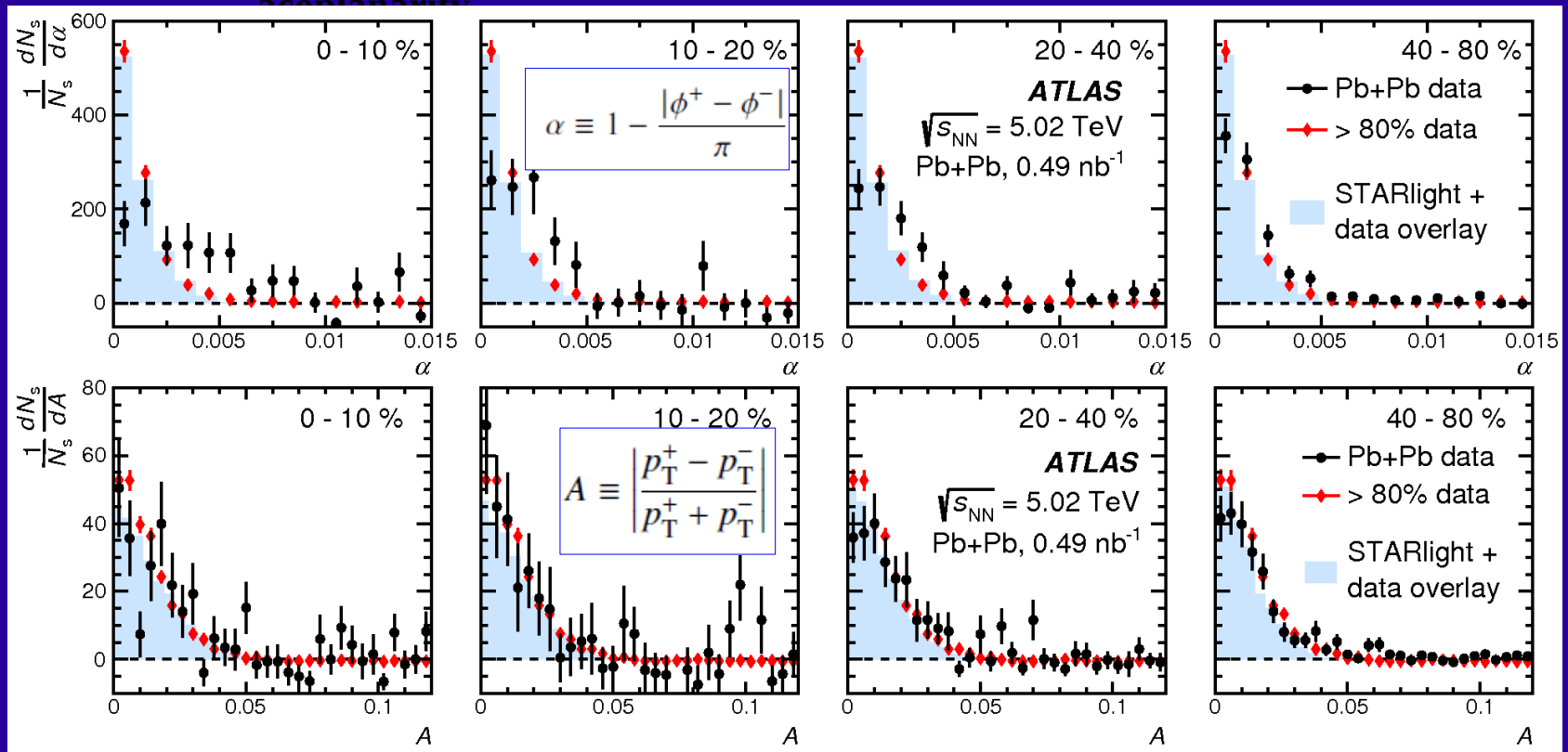
Stay tuned for Pb+Pb 2018 data analysis (more than factor 2 statistics) and LHC Run 4 with increased tracking acceptance.



$\gamma\gamma \rightarrow \mu^+\mu^-$ in non-UPC

Phys. Rev. Lett. 121 (2018) 212301

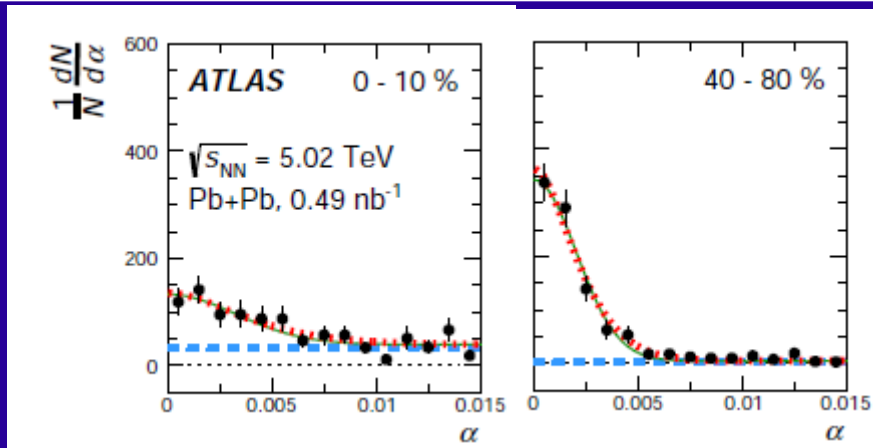
Dimuon pairs resulting from photonuclear interactions occurring simultaneously with the hadronic collision.



- Data reveals balance in energy, but acoplanarity broadening with centrality.
- STARlight agrees in peripheral, but not in central collisions.

$\gamma\gamma \rightarrow \mu^+\mu^-$ in non-UPC

Phys. Rev. Lett. 121 (2018) 212301



if broadening results from small k_T transfer:

$$\langle \alpha^2 \rangle = \langle \alpha^2 \rangle_0 + \frac{1}{\pi^2} \frac{\langle \vec{k}_T^2 \rangle}{\langle P_{T \text{ avg}}^2 \rangle}$$

Centrality	$\langle N_{\text{part}} \rangle$	$p_{T \text{ avg}}^{\text{RMS}}$ [GeV]	Gaussian fit			Convolution fit
			$\sigma_A (\times 10^3)$	$\sigma_\alpha (\times 10^3)$	k_T^{RMS} [MeV]	k_T^{RMS} [MeV]
0–10%	359 ± 2	7.0 ± 0.1	$17.9^{+1.0}_{-0.9}$	3.3 ± 0.4	66 ± 10	70 ± 10
10–20%	264 ± 3	7.7 ± 0.4	$13.6^{+1.2}_{-1.0}$	2.3 ± 0.3	40 ± 7	42 ± 7
20–40%	160 ± 3	7.4 ± 0.3	$17.2^{+0.4}_{-0.4}$	2.5 ± 0.2	48 ± 6	44 ± 5
40–80%	47 ± 2	6.8 ± 0.3	$16.1^{+0.1}_{-0.1}$	2.0 ± 0.1	35 ± 4	32 ± 2
> 80%	–	7.0 ± 0.3	$15.5^{+0.1}_{-0.1}$	1.40 ± 0.03	–	–

- Modifications are qualitatively consistent with re-scattering of the muons while crossing the QGP.

Electroweak probes in p+Pb collisions – γ

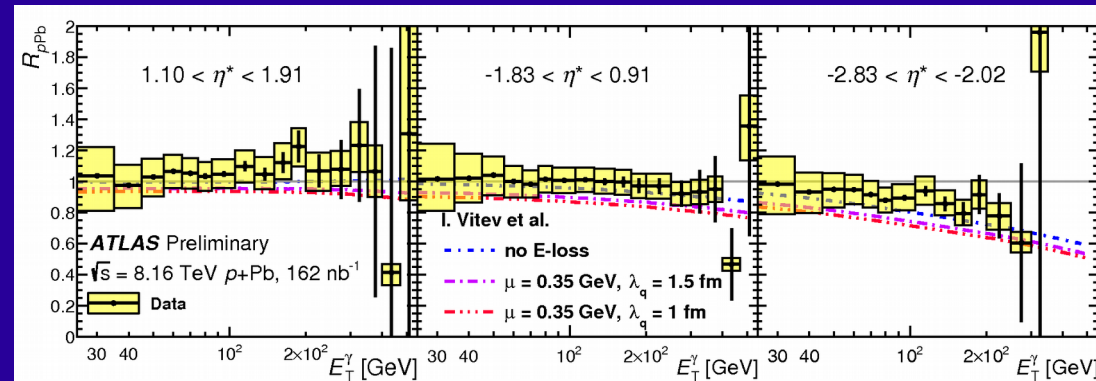
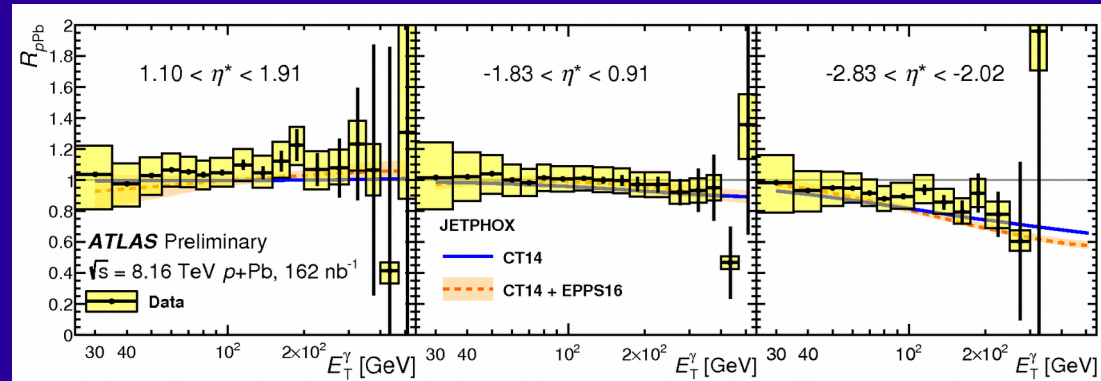
- Inclusive prompt photons in p+Pb collisions at 8.16 TeV.

$$E_T^\gamma > 25 \text{ GeV}$$

$$E_T^{\text{iso}} < 4.8 \text{ GeV} + 4.2 \times 10^{-3} E_T^\gamma \text{ [GeV]}$$

- R_{pPb} consistent with unity at central and forward rapidity.
- $R_{pPb} < 1$ for $\eta^* < -2$ due to isospin effects.
- Data consistent within uncertainties with both free nPDF and with the small effects expected from a nuclear modification of the parton densities.

- Data disfavors large suppression due to E-loss.

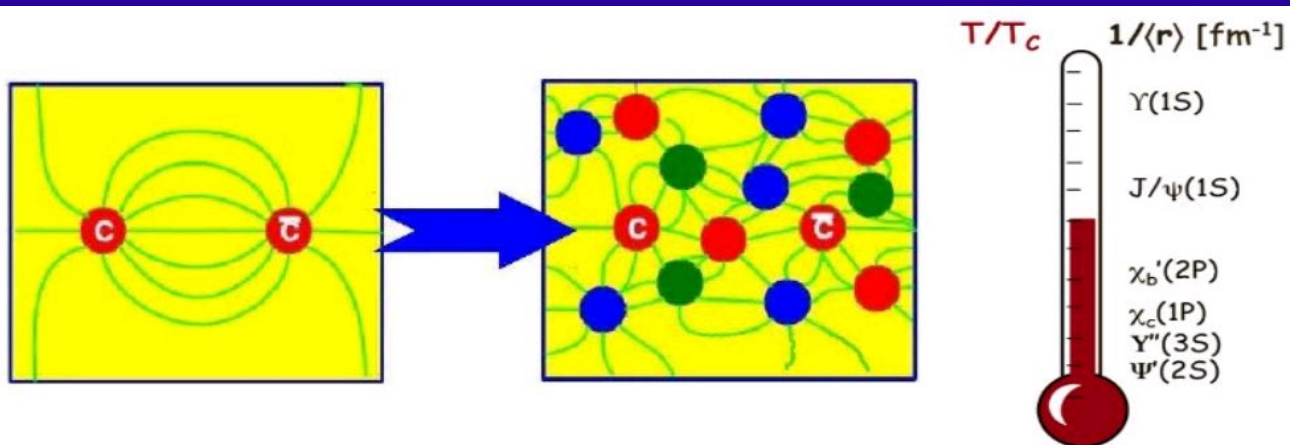


Messages from EW

- Photons, Z and W^\pm productions consistent with expectations from T_{AA} scaling.
- No visible modifications of nuclear PDFs within uncertainties.
- Evidence of LbyL scattering: 4.4 (3.8) σ .
- Modifications in the acoplanarity of dimuons produced in non-UPC by magnetic fields are qualitatively consistent with re-scattering while crossing the QGP.

Quarkonia

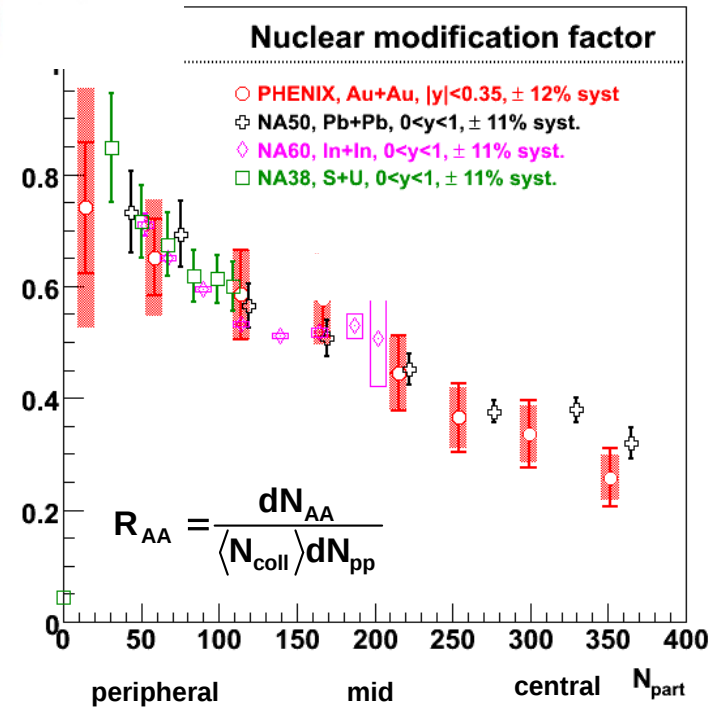
Quarkonia suppression is predicted by lattice QCD calculations



J/ψ anomalous suppression by Debye colour screening (Matsui and Satz, 1986)

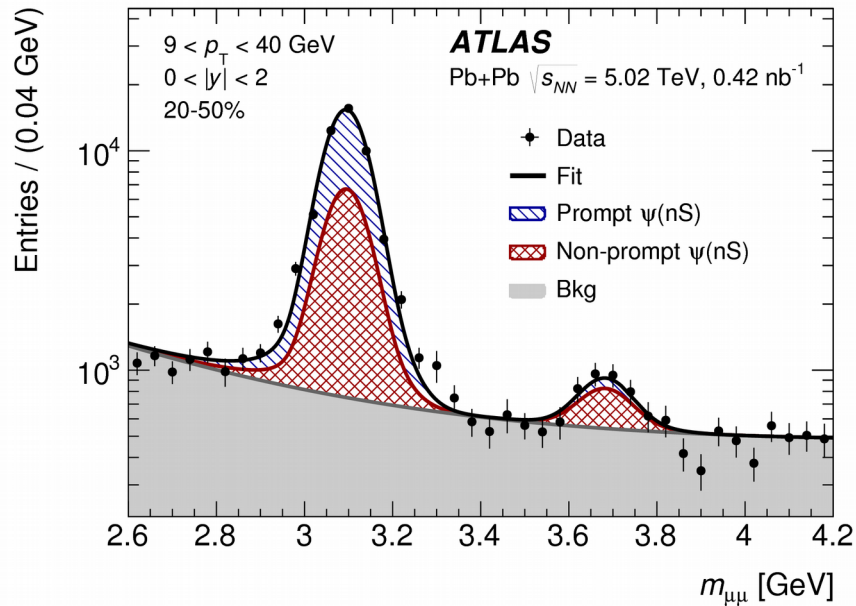
→ One of the most striking signatures for the QGP

→ A major contribution from LIP

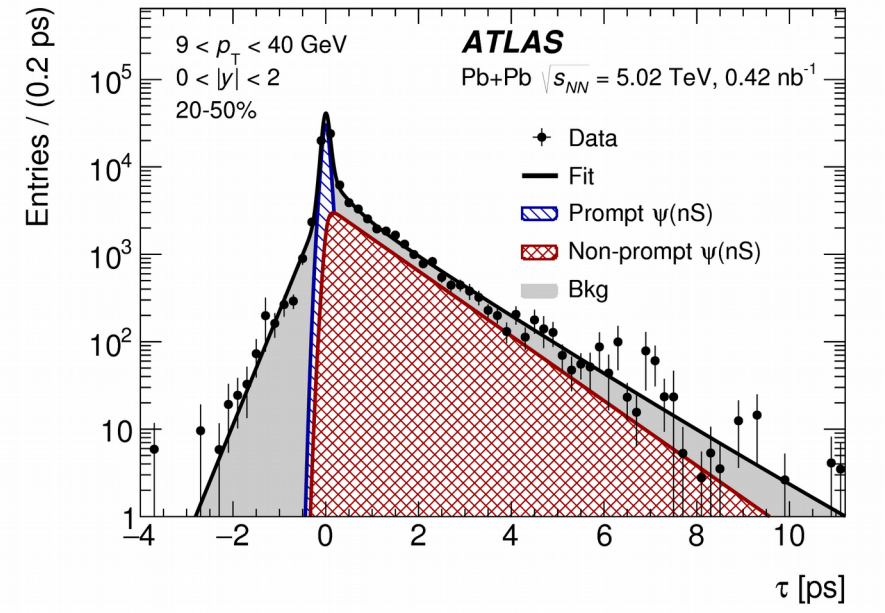


Prompt and Non-prompt Charmonia in Pb+Pb ¹⁸

Dimuon invariant mass



Dimuon pseudo-proper time

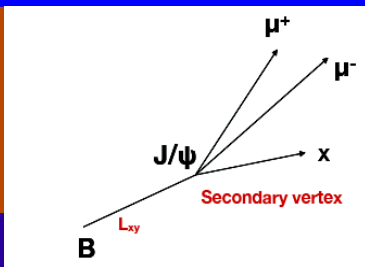
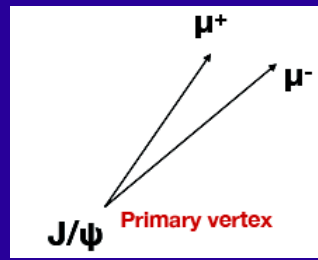


Prompt J/ψ: direct production; feed-down from excited states.

Modified by colour screening and regeneration in the QGP.

Non-prompt J/ψ: decays from B-hadrons

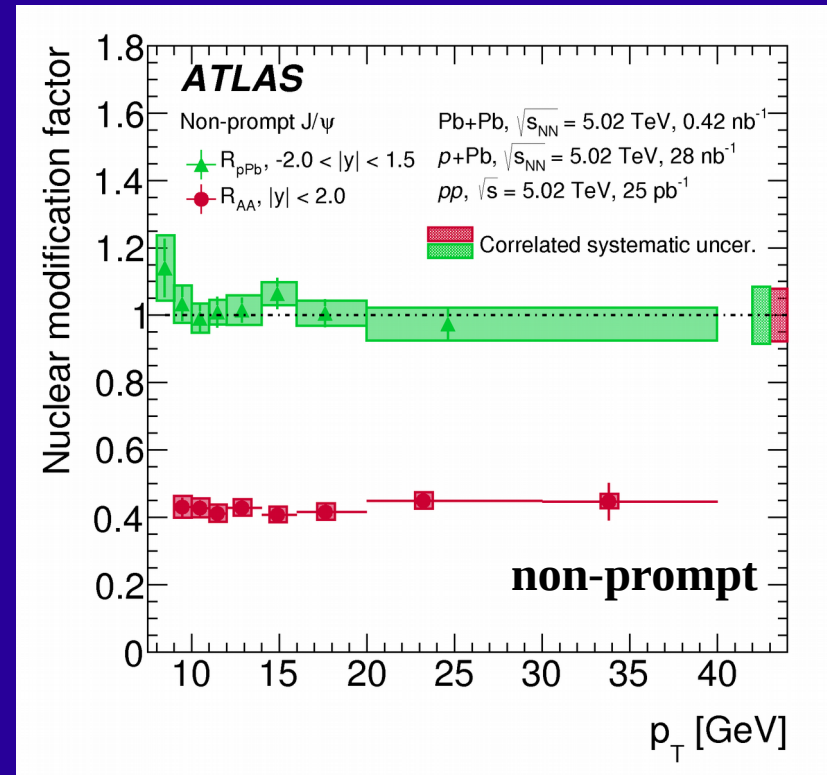
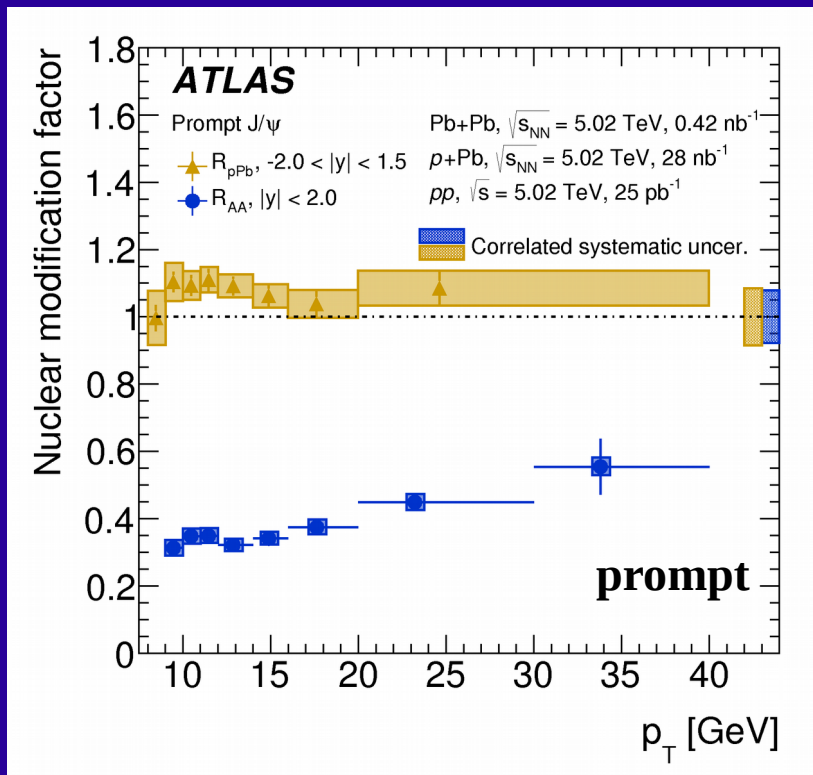
Energy loss of the b-quarks in the QGP.



$$\tau = \frac{L_{xy} m_{\mu\mu}}{p_T^{\mu\mu}}$$

J/ψ R_{pPb} and R_{AA} as a function of p_T

Quarkonia in p+Pb collisions is a probe of cold nuclear matter effects



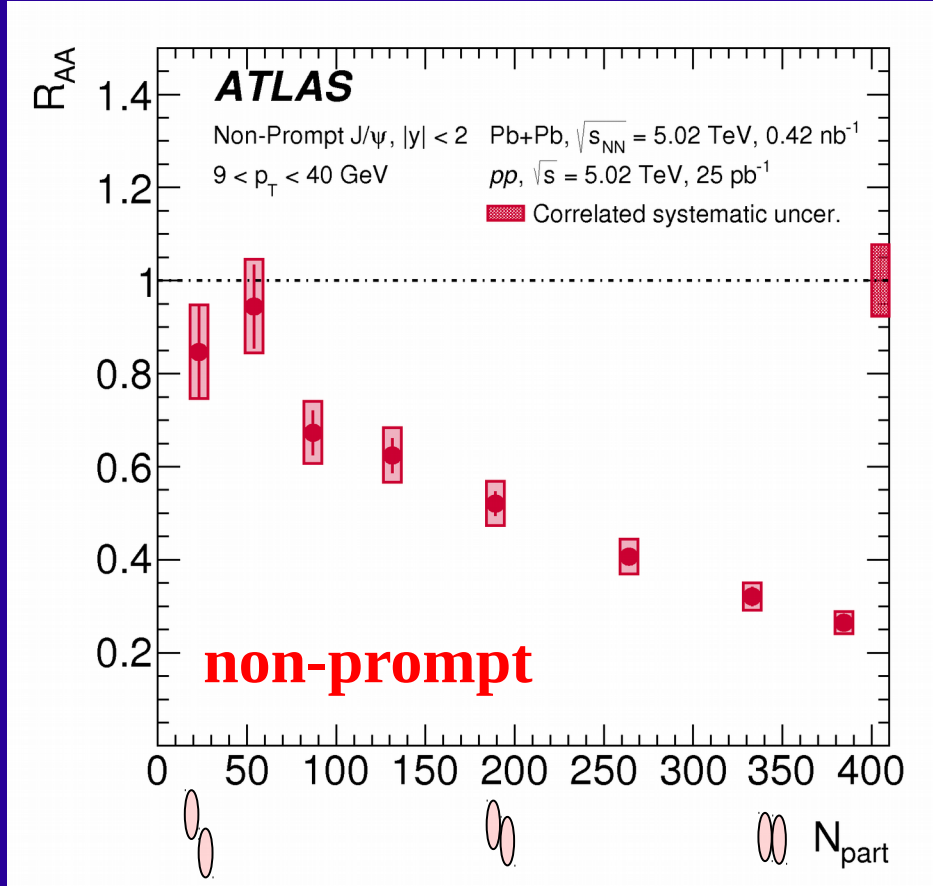
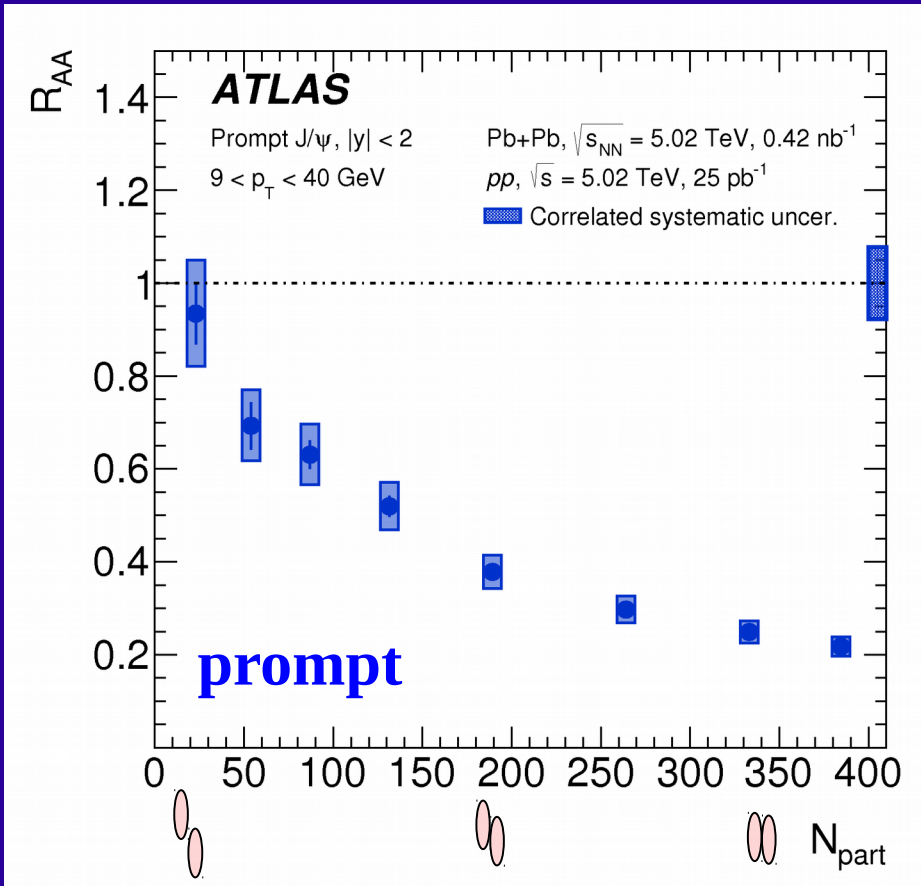
- R_{pPb} is consistent with unity.

$$R_{pPb} = \frac{1}{208} \frac{\sigma_{p+Pb}^{O(nS)}}{\sigma_{pp}^{O(nS)}}$$

- J/ψ is strongly suppressed in Pb+Pb; prompt and non-prompt mechanisms have different p_T dependence.

J/ψ R_{AA} as a function of N_{part}

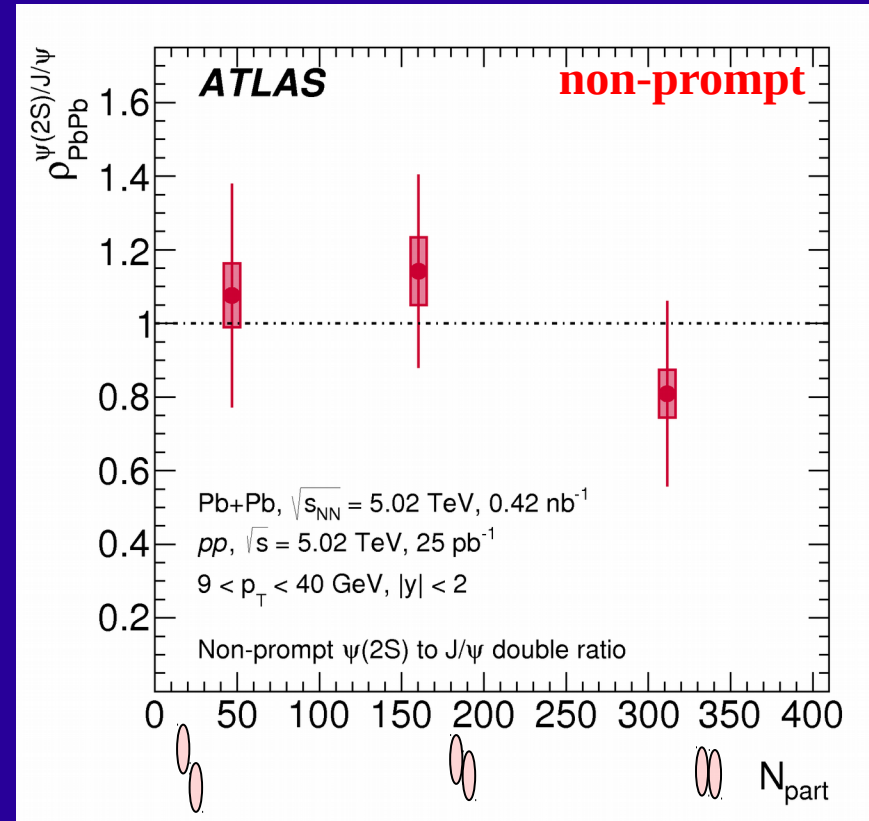
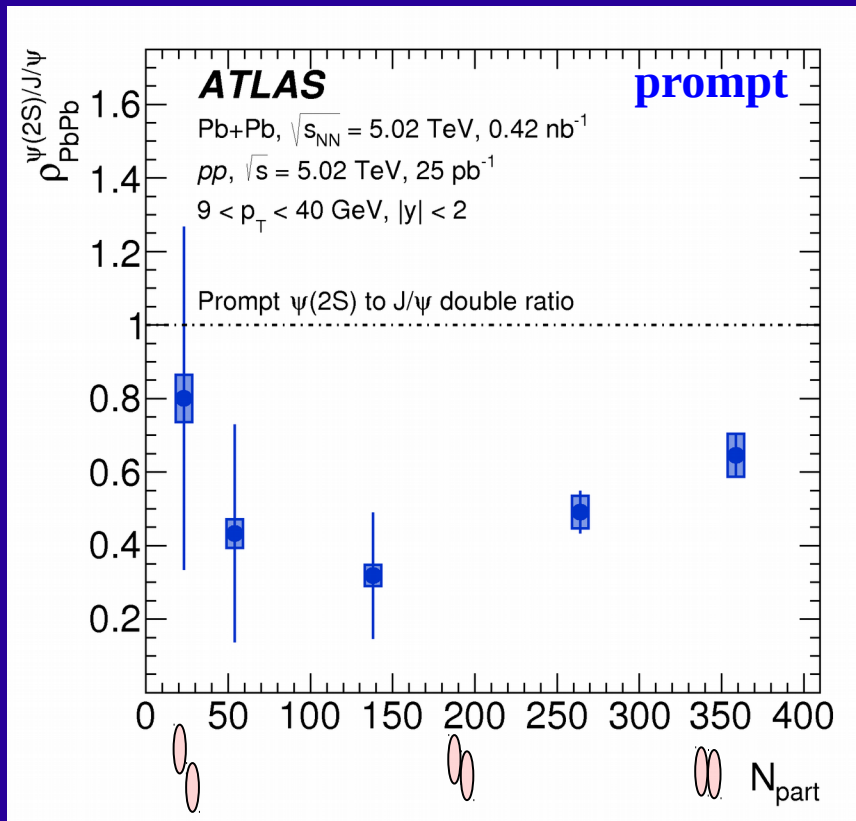
Eur. Phys. J. C 78 (2018) 762



Strong centrality dependence for both **prompt** and **non-prompt** J/ψ ,
 with similar suppression pattern.

$\psi(2S)$ to J/ψ as a function of N_{part}

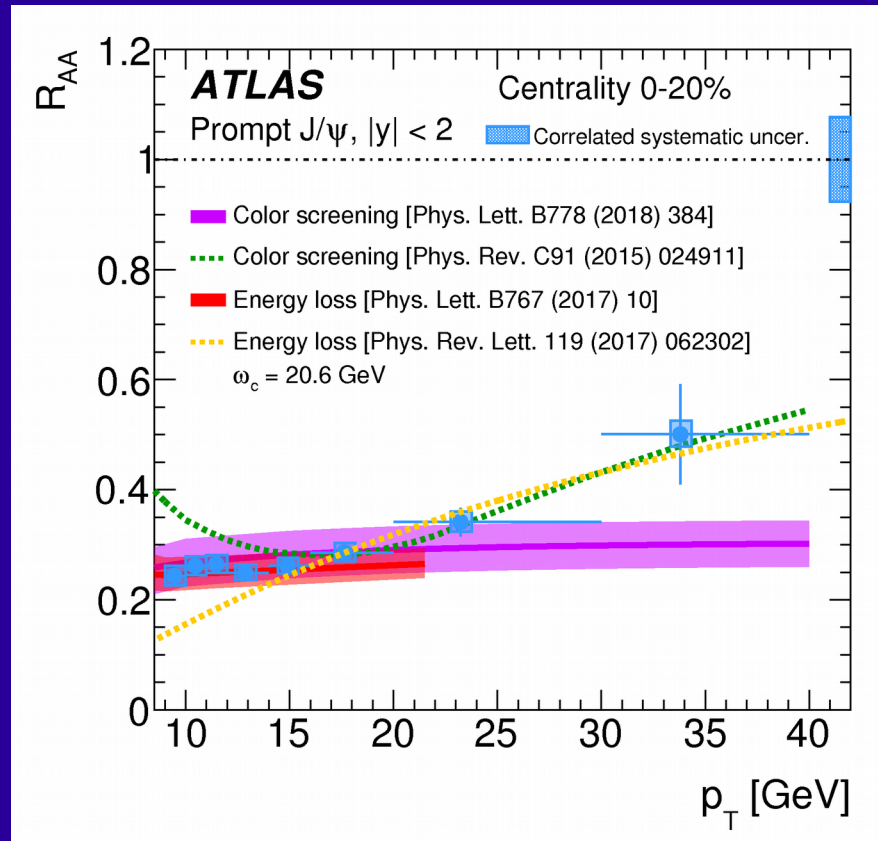
Eur. Phys. J. C 78 (2018) 762



- Prompt $\psi(2S)$ to J/ψ ratio increases in central collisions, supporting the hypothesis of $\psi(2S)$ being produced by regeneration. More data is needed.
- Non-prompt $\psi(2S)$ to J/ψ ratio is consistent with unity, suggesting that both mesons originate from b-quarks hadronising outside the QGP.

Prompt J/ψ R_{AA} as a function of p_T

Eur. Phys. J. C 78 (2018) 762

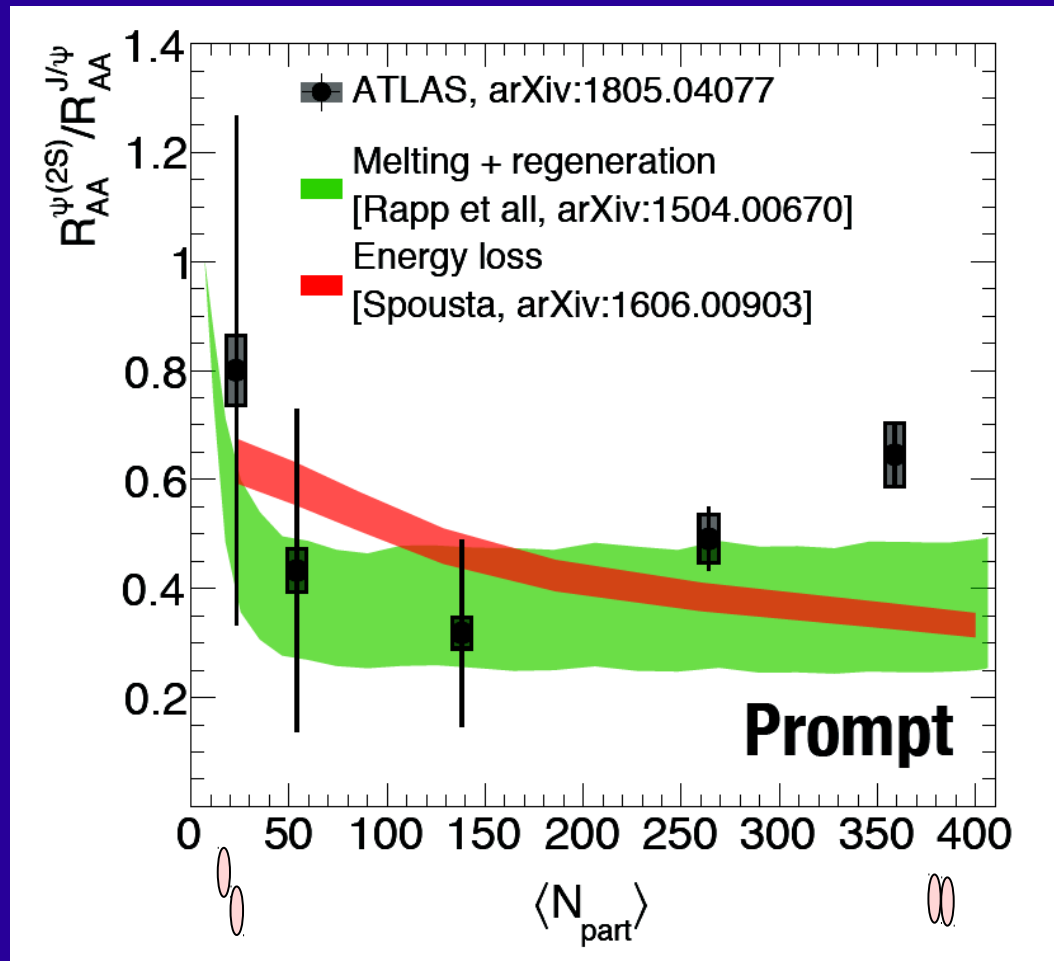


Data at high p_T well described by **color screening** and **energy loss** scenarios, but they miss low p_T .

Different models on **color screening** and **energy loss** agree at low p_T , but fail at high p_T .

Prompt $\psi(2S)$ to J/ψ as a function of N_{part}

Eur. Phys. J. C 78 (2018) 762



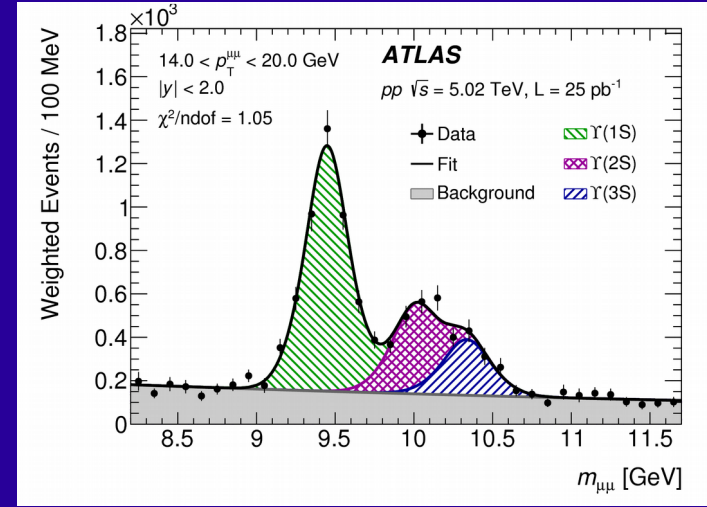
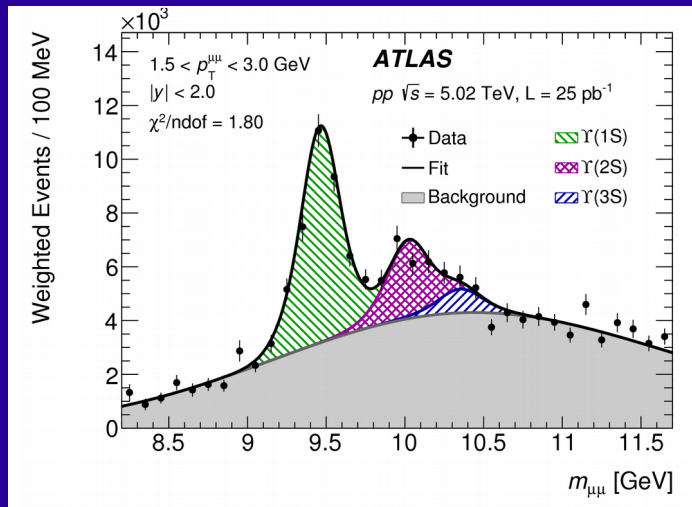
Both models foresee the decrease in the double ratio, but fail in describing simultaneously all centralities.

Bottomonium Fits to Dimuon Invariant Mass

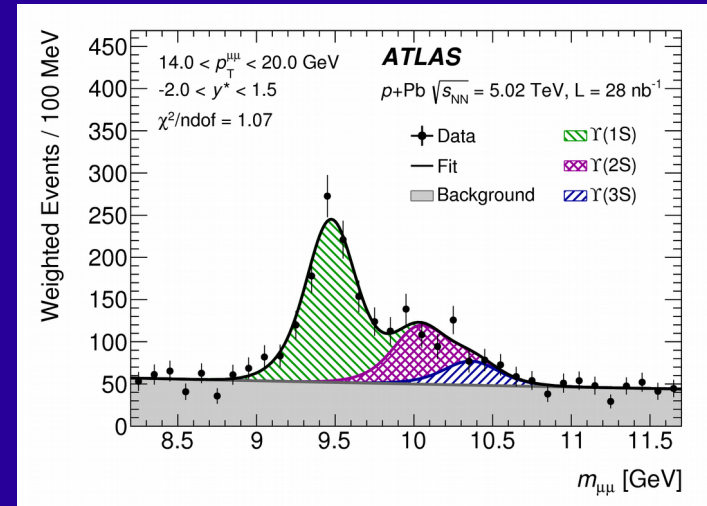
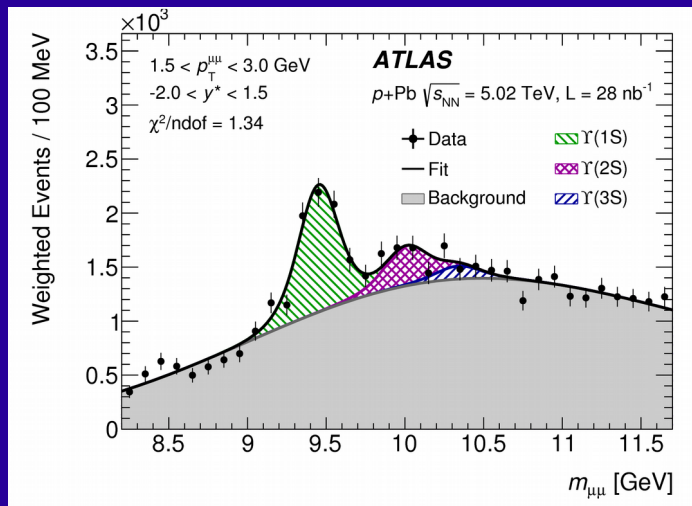
$1.5 < p_T < 3.0$ GeV

$14.0 < p_T < 20.0$ GeV

pp



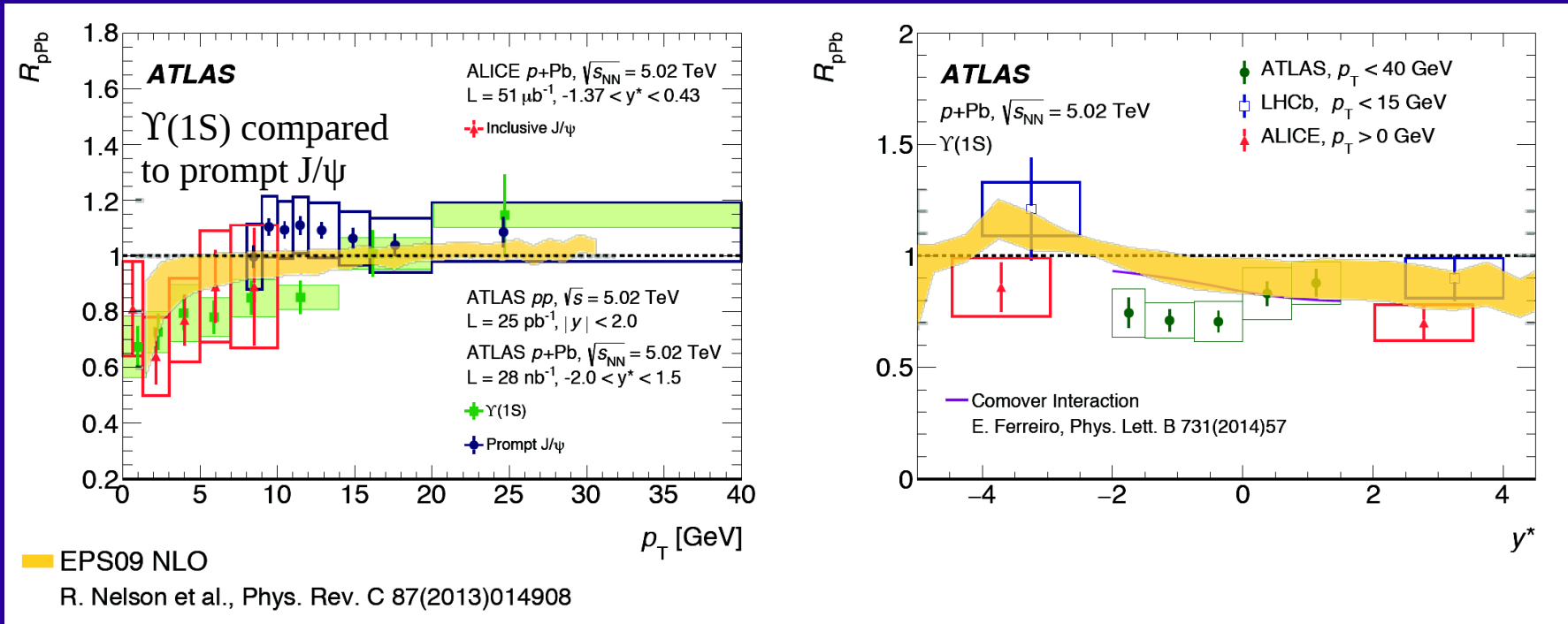
p+Pb



Quarkonia R_{pPb} as a function of p_T and y^*

Eur. Phys. J. C 78 (2018) 171

$p+Pb$ collisions are important to disentangle effects due to quarkonium interactions with QGP from those attributed to CNM.



- R_{pPb} is consistent with unity for $p_T > 9$ GeV \rightarrow important reference for the suppression at high p_T in larger collision systems (Pb+Pb and Xe+Xe).
- Models provide qualitatively good description.

Messages from Quarkonia

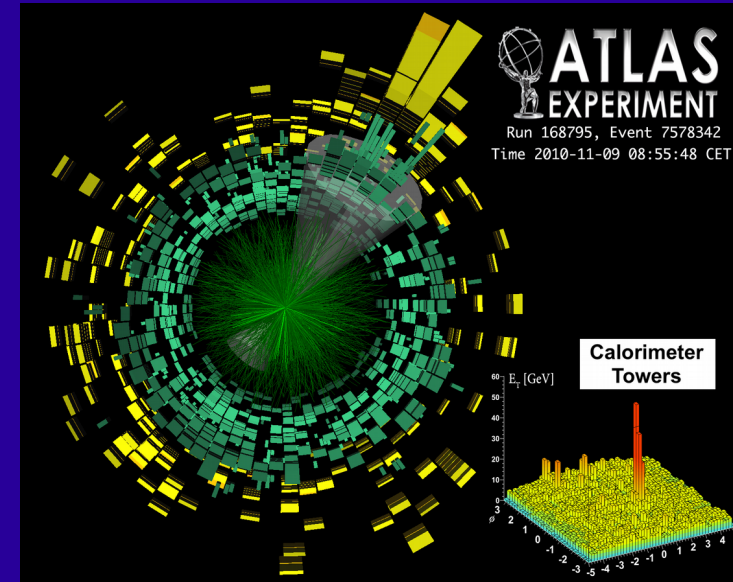
- Strong centrality dependence, and with similar suppression, for both prompt and non-prompt J/ψ .
- **Modest dependence on $|y|$ (in backup). Different p_T dependence.**
- Data at high p_T well described by color screening and energy loss models. But these miss low p_T .
- **Indications of prompt $\psi(2S)$ regeneration in central collisions.**
- Non-prompt $\psi(2S)$ to J/ψ ratio is consistent with unity.
- **$\Upsilon(1S)$ and J/ψ R_{pPb} is consistent with unity for $p_T > 9$ GeV.**

Jets as probes of hot matter

QGP is opaque to coloured partons. How do parton showers in the hot and dense medium differ from those in vacuum?

What is expected:

- Partons lose energy, resulting in jet “quenching”.
- Jets probe the very first phase of the collision
→ they carry relevant information about the QGP.



Different observables allow to disentangle the nature of the Eloss:

Dijet Asymmetry, Acoplanarity

Correlation with colour neutral probes (Z and photons)

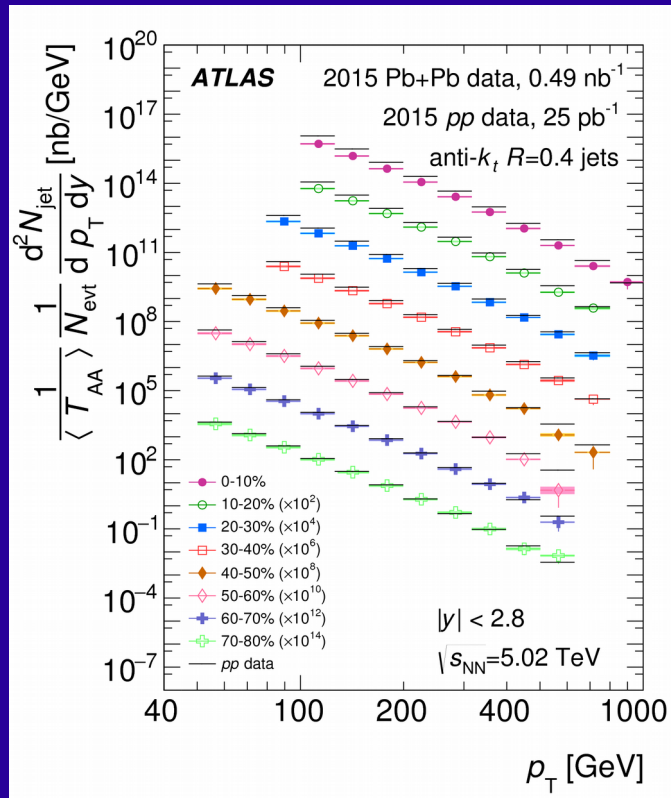
Differential inclusive jet suppression

Jet structure and properties of quenched jets

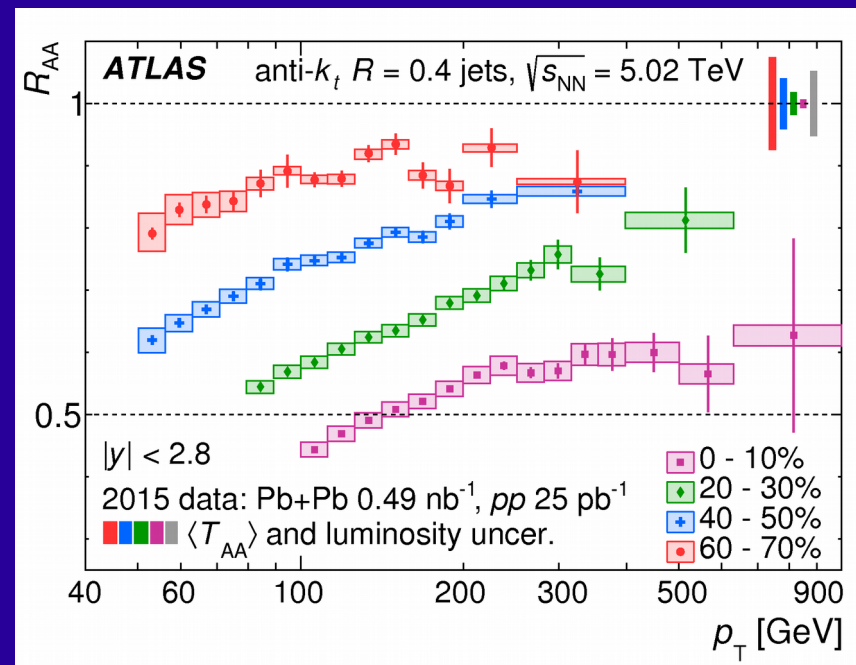
Inclusive jet production in Pb+Pb

arXiv:1805.05635

Per event jet yields in Pb+Pb collisions, divided by $\langle T_{AA} \rangle$, as a function of jet p_T for different centrality intervals.

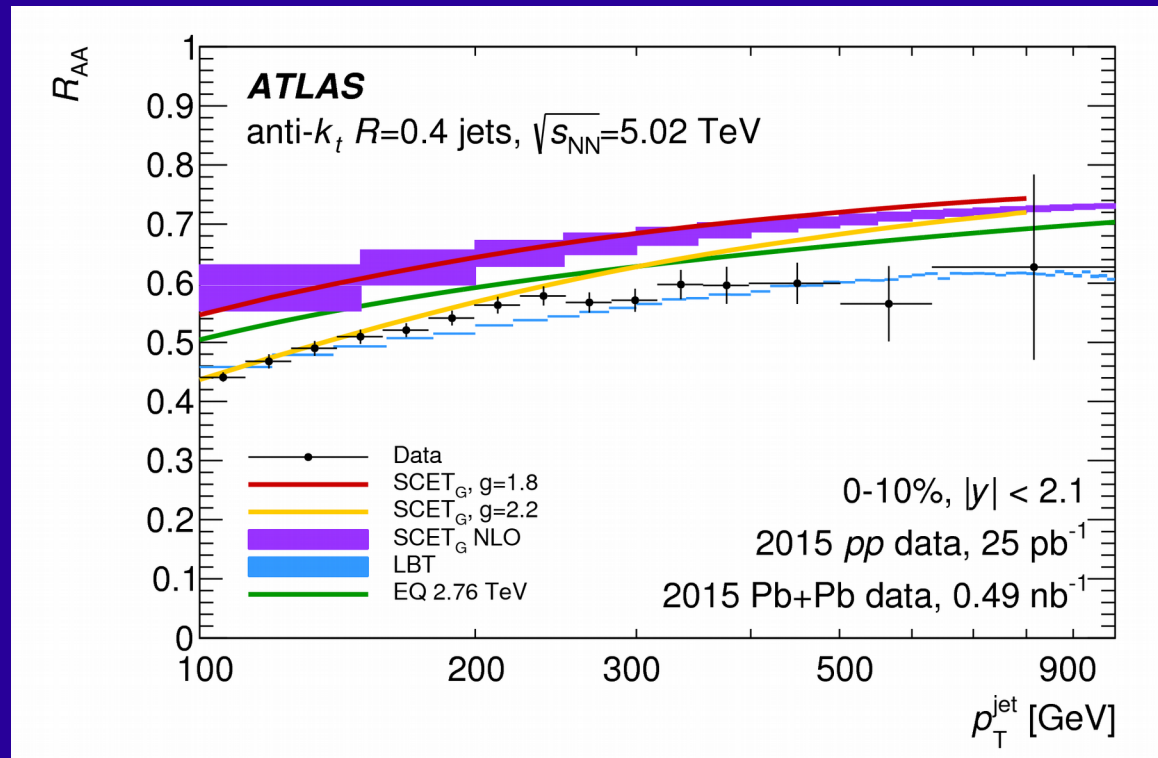


Jet R_{AA} as a function of p_T for different centrality intervals.



- Jets are suppressed by a factor of two in central Pb+Pb collisions with clear dependence on transverse momentum, p_T .
- Peripheral collisions (60 – 70%) show also significant suppression.

Jet R_{AA} compared with theory



[Linear Boltzmann Transport \(LBT - 1503.03313\)](#)

[Soft Collinear Effective Field Theory \(SCETg - 1509.02936\)](#)

[Effective Quenching \(EQ - 1504.05169\)](#)

All models reproduce the trend shown by the data. EQ and SCETg (with exception for $g=2.2$) clearly underestimate the suppression.

$R_{AA}^{|y|}$ to the $R_{AA}^{|y|<0.3}$ as a function of $|y|$

Two effects competing

(1504.05169):

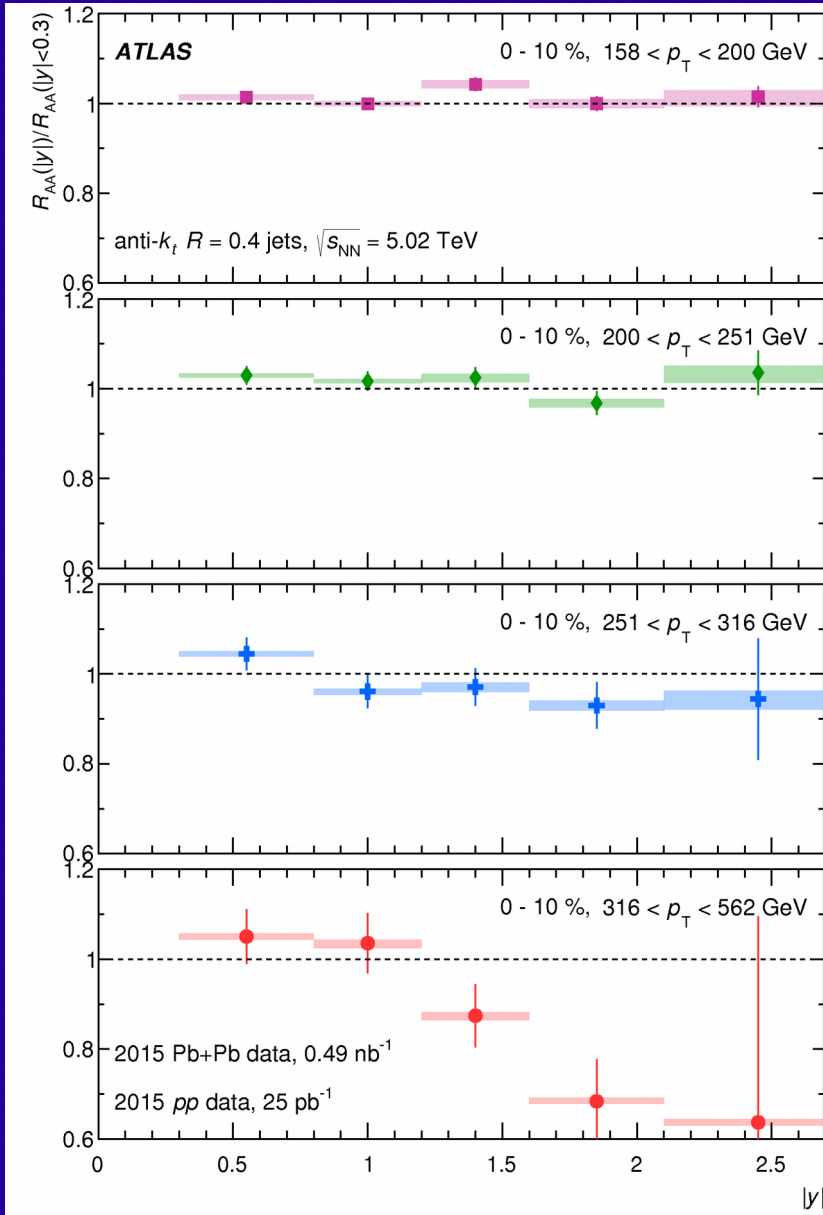
1 - Fraction of quark jets increases with $|y|$ at fixed jet p_T ; Quarks should lose less energy than gluons

→ Increase R_{AA} with $|y|$

2 - Spectra become steeper with increasing $|y|$

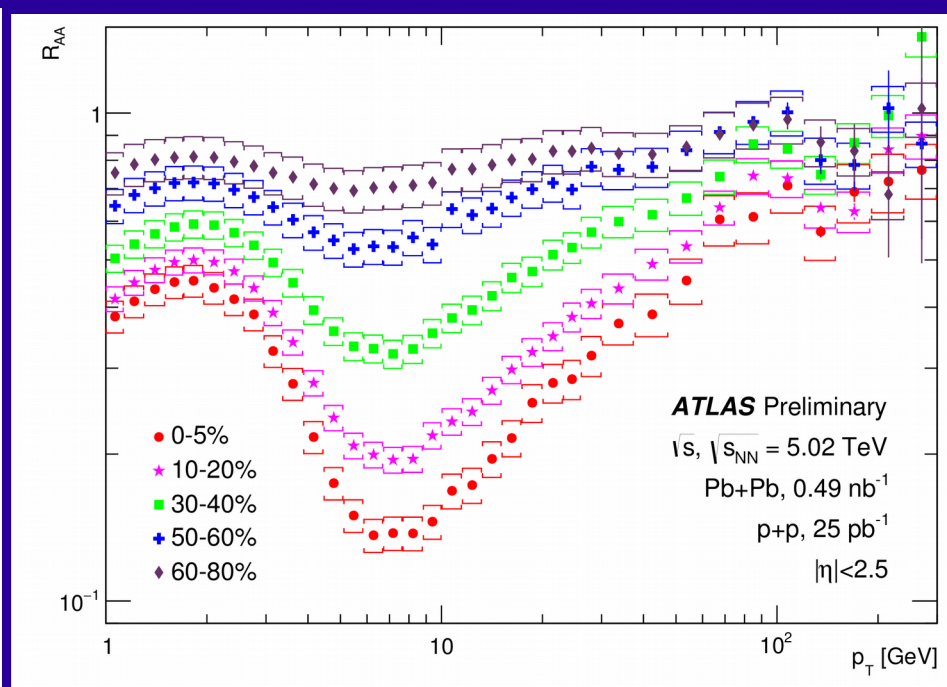
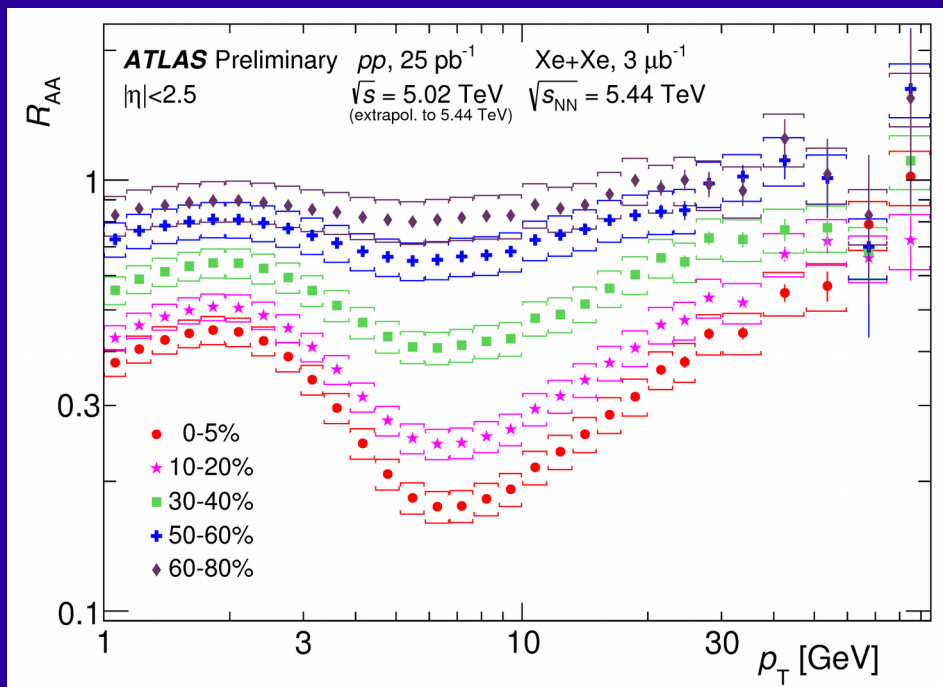
→ Decrease R_{AA} with $|y|$

For high p_T the effect of the steeper spectra dominates.



Charged Hadron R_{AA} in Xe+Xe and Pb+Pb³¹

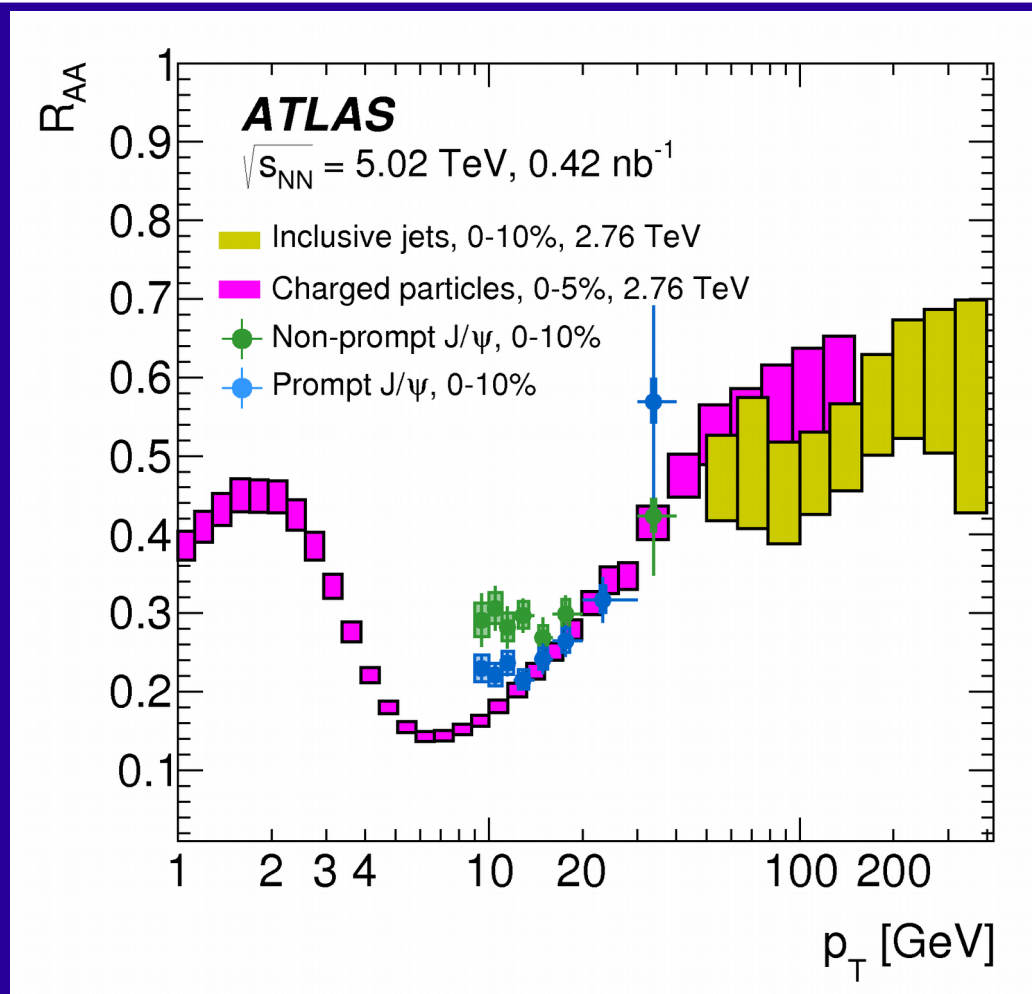
ATLAS-CNF-2018-007



Note different x-axis

Qualitatively similar

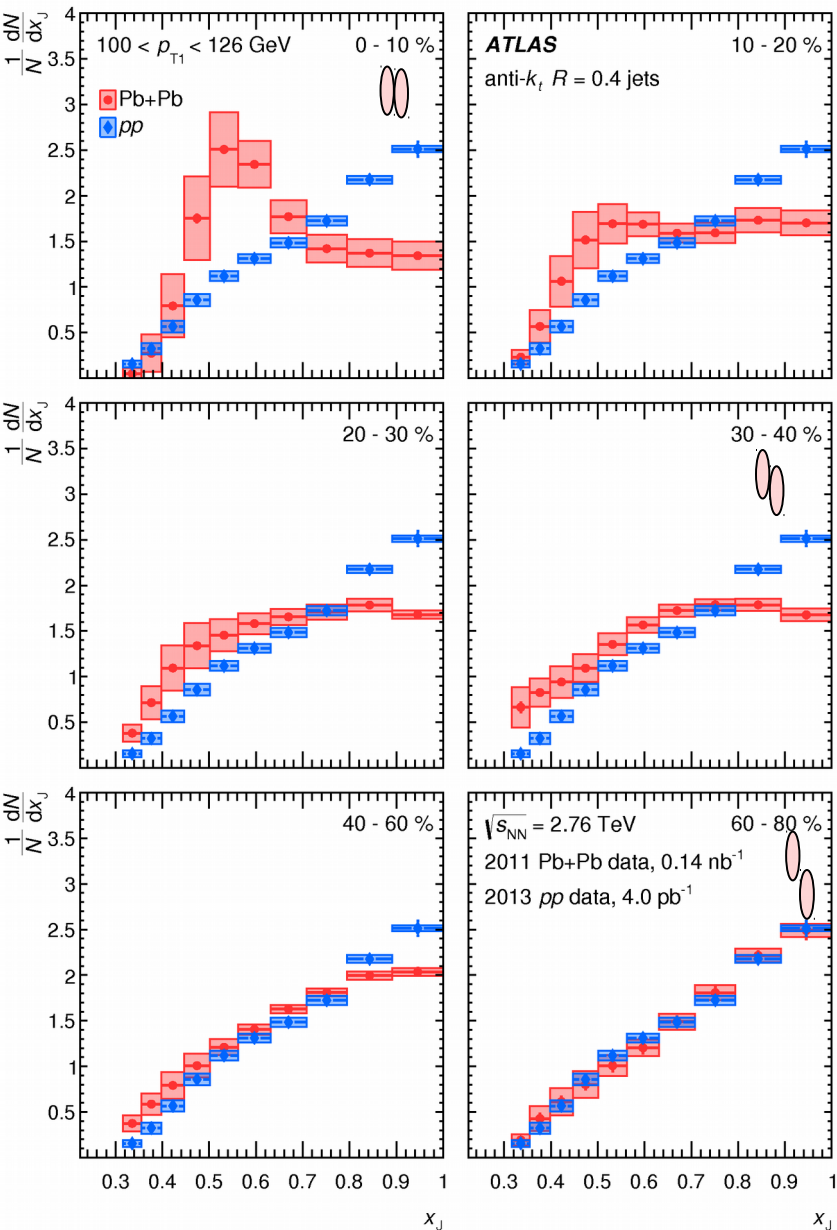
R_{AA} as a function of p_T in different channels



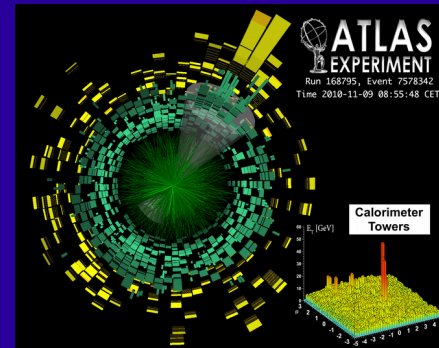
Suggestion of high p_T universality from suppression of several different probes \rightarrow prompt J/ ψ may also be sensitive to parton energy loss.

Dijet asymmetry in Pb+Pb and pp collisions

arXiv:1706.09363 [hep-ex]



Centrality dependence of
 $x_J = p_{T2}/p_{T1}$ for jet
 $100 < p_{T1} < 126$ GeV



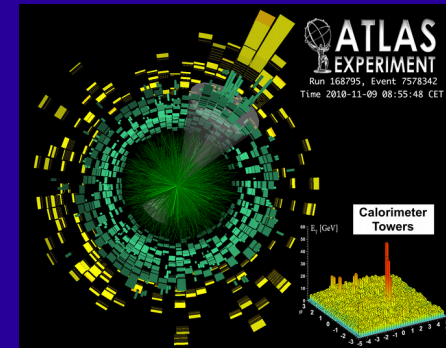
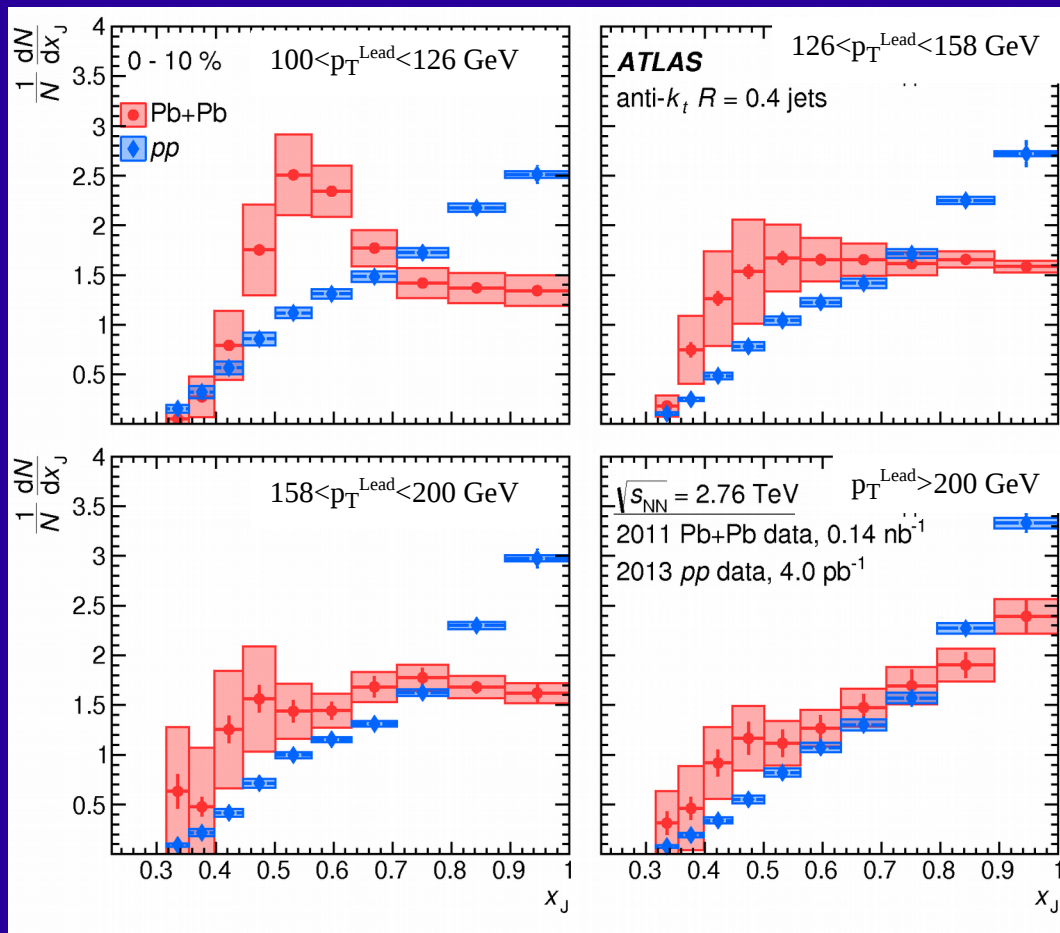
Dijet asymmetry probes
differences in quenching between
the two parton showers.

- ★ The asymmetry in peripheral collisions is well compatible with pp collisions
- ★ The asymmetry increases with collision centrality

Dijet asymmetry in Xe+Xe and pp collisions

arXiv:1706.09363 [hep-ex]

p_{T1} dependence of $x_J = p_{T2}/p_{T1}$ in central collisions



Discrepancy between Pb+Pb and pp dilutes with increasing p_{T1} .

Much smaller modification at high p_{T}^{Lead} .

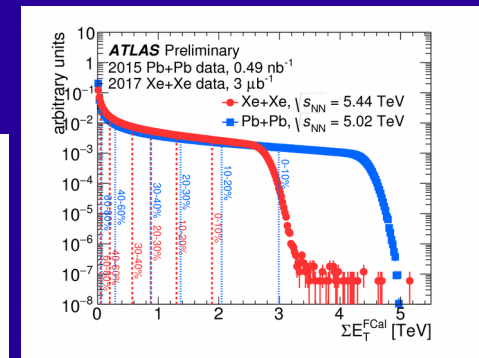
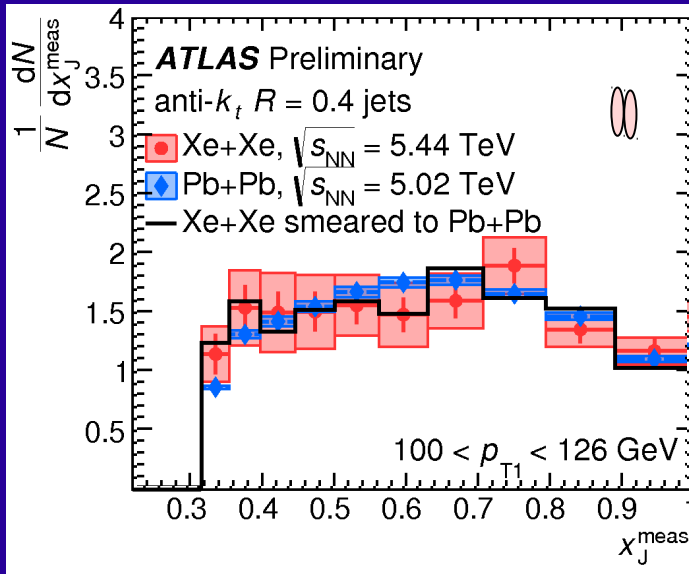
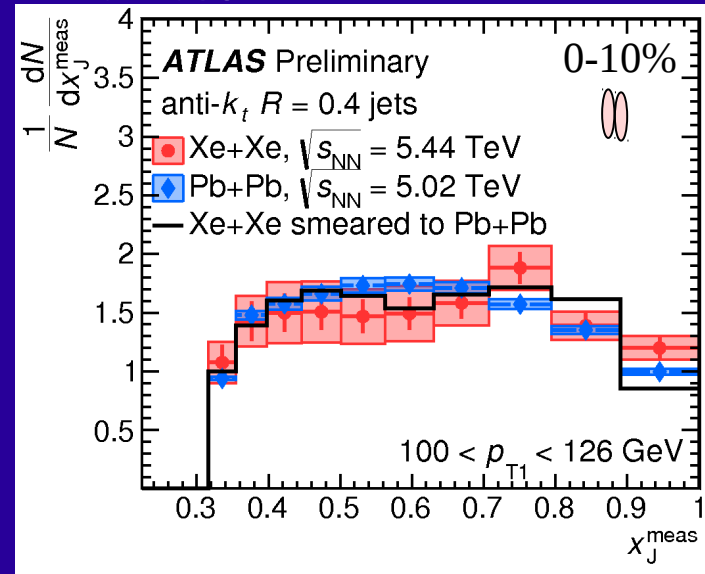
Leading contribution from LIP ATLAS group

Dijet asymmetry in Xe+Xe and Pb+Pb

ATLAS-CONF-2018-007

Same collision centrality,
0-10%

Same ΣE_T^{FCal} range
 $2.05 < \Sigma E_T^{\text{FCal}} < 2.99$ TeV



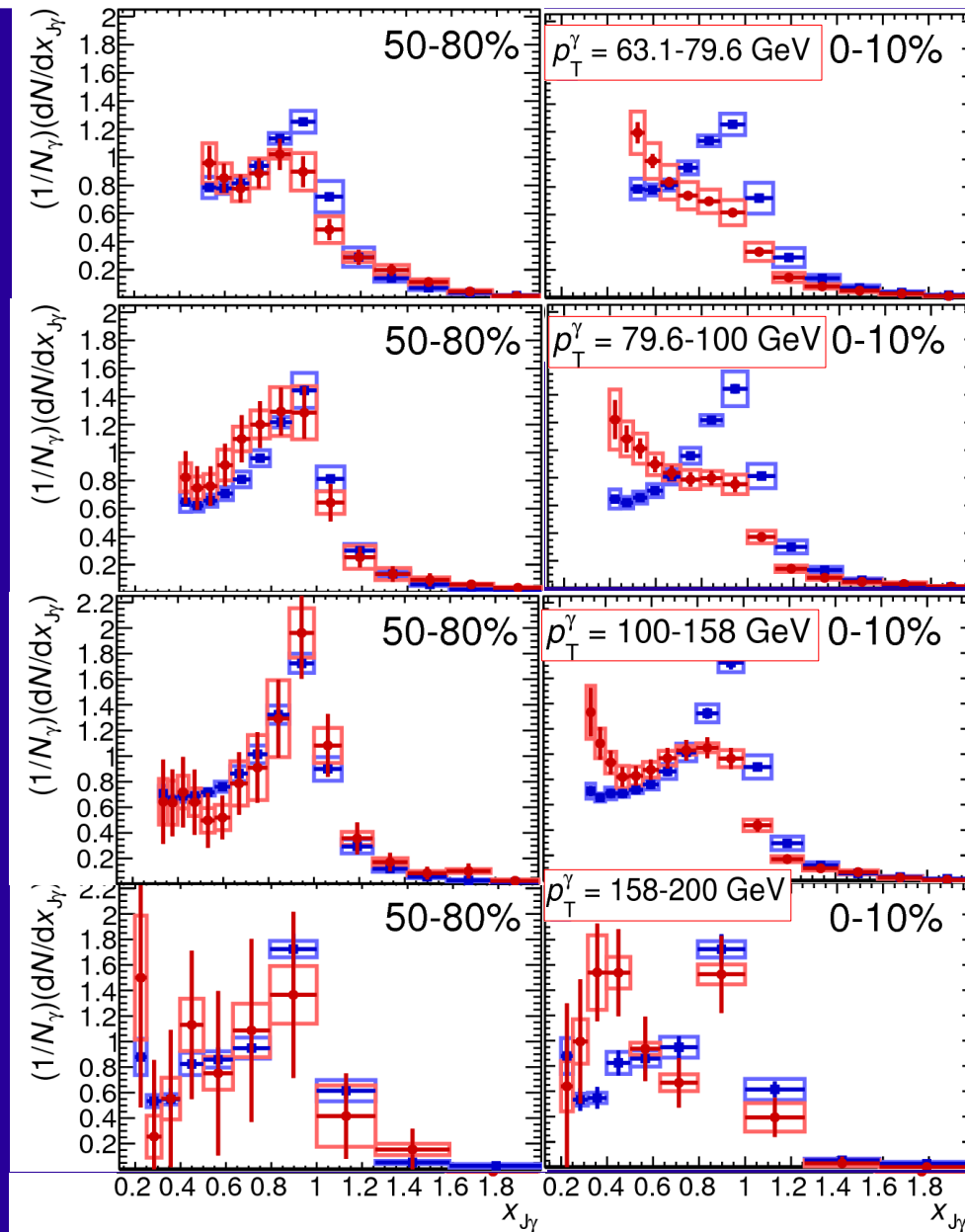
Both Xe+Xe and Pb+Pb results are not corrected for detector effects. Black line represents Xe+Xe smeared to Pb+Pb.

→ Difference in underlying event fluctuations has minimal impact in the result.

Consistency between Xe+Xe and Pb+Pb in both centrality and ΣE_T^{FCal} ranges.

No dependence on geometry of the collision within uncertainties.

Electroweak probes: γ + jet p_T balance



ATLAS

pp 5.02 TeV, 25 pb⁻¹

Pb+Pb 5.02 TeV, 0.49 nb⁻¹

■ pp (same each panel)

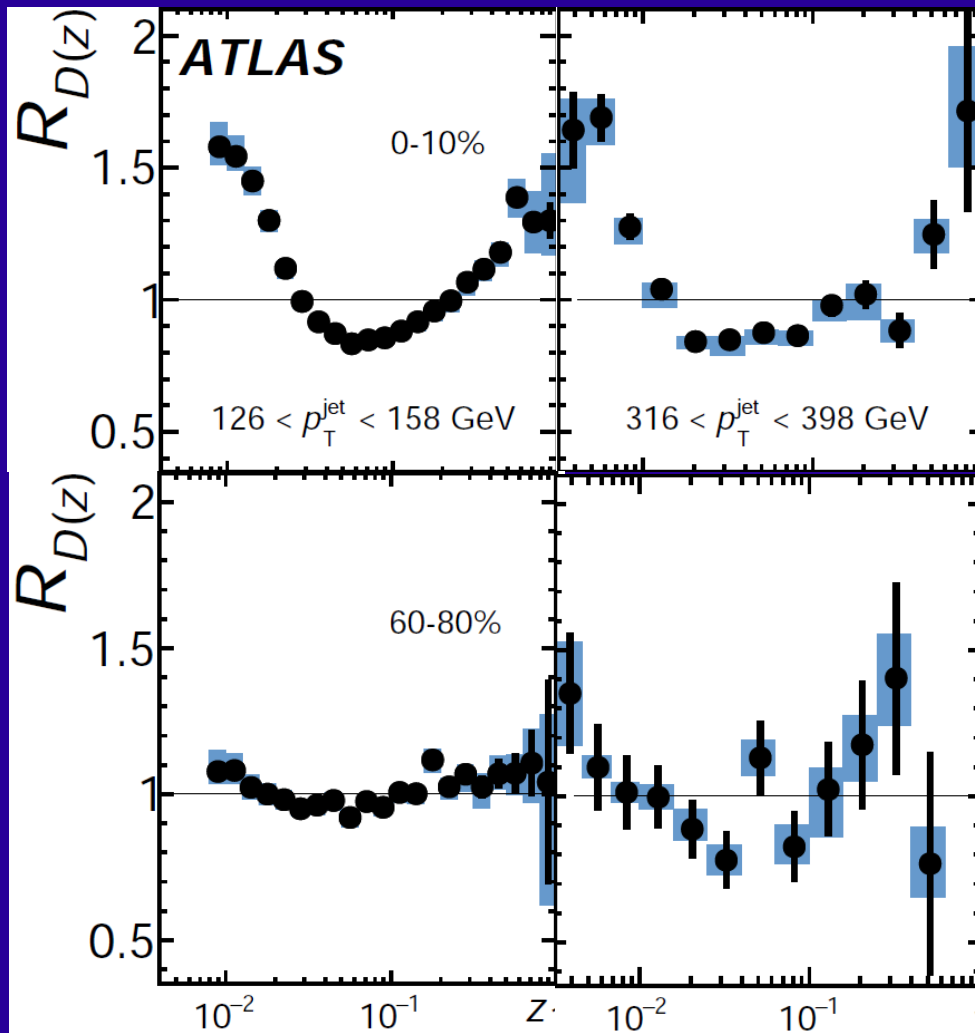
● Pb+Pb

Fully corrected for detector effects

- pp-like peaked $x_{J\gamma} = p_T^J/p_T^\gamma$, independently of jet p_T , in peripheral Pb+Pb.
- Increasing double peak shape with jet p_T in central.

Jet structure

Phys. Rev. C 98 (2018) 024908



A diagram showing several yellow arrows originating from a common point. One arrow is vertical, representing the jet axis. Other arrows point in various directions, representing particles within the jet. A dashed vertical line indicates the projection of the jet axis onto the direction of a particle.

$$z \equiv \frac{p_T}{p_T^{\text{jet}}} \cos \Delta R$$

$$D(z) \equiv \frac{1}{N_{\text{jet}}} \frac{dN_{\text{ch}}}{dz}$$

$$R_{D(z)} = D(z)_{\text{cent}} / D(z)_{\text{p+p}}$$

Internal jet structure shows enhancement of particle yields at low z ; enhancement at high z ; depletion at intermediate.

Messages from Jets

- Inclusive jets in Pb+Pb are suppressed relatively to p+p up to a factor of 2.
- Hadrons also suppressed (as expected), with characteristic dependence on the transverse momentum.
- Internal jet structure shows enhancement of particle yields at low z ; enhancement at high z , depletion at intermediate.
- Enhancement of asymmetric dijets in Xe+Xe and Pb+Pb, relatively to p+p as the centrality increases.
- Clear dependence with the p_T of the leading.

Outlook

Stay tuned to the results provided by the $1.75^{-\text{nb}}$ recorded by ATLAS during 2018 Pb+Pb @ 5.02 TeV data acquisition. A factor of 3.5 w.r.t. 2015.

Peak luminosity of $6 \times 10^{27} \text{ cm}^{-2} \text{ s}^{-1}$ reached several times

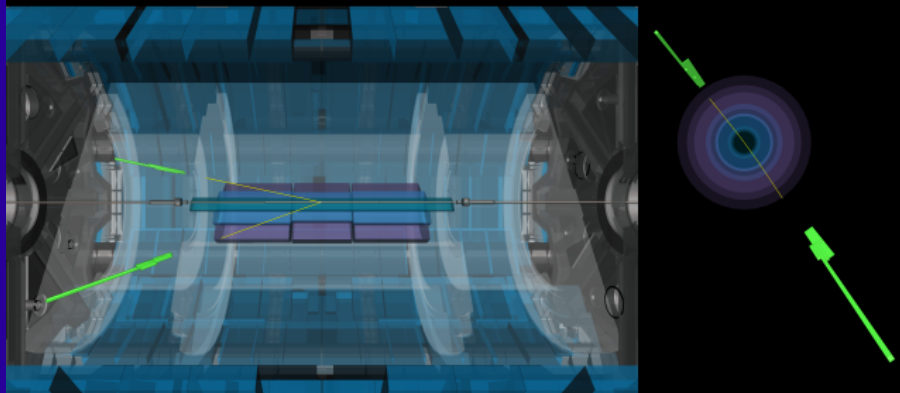
=> good prospects for the Run 3.

See Agnieszka Ogrodnik's talk tomorrow.



Run: 365512
Event: 130954442
2018-11-09 07:56:44 CEST

$p_T^{e1} = 8.2 \text{ GeV}$
 $p_T^{e2} = 7.4 \text{ GeV}$



$\gamma\gamma \rightarrow ee$ candidate in ultra-peripheral collision in 2018 Pb+Pb dataset. $p_T(e_1) = 8.2 \text{ GeV}$ and $p_T(e_2) = 7.4 \text{ GeV}$; $m_{ee} = 16 \text{ GeV}$.

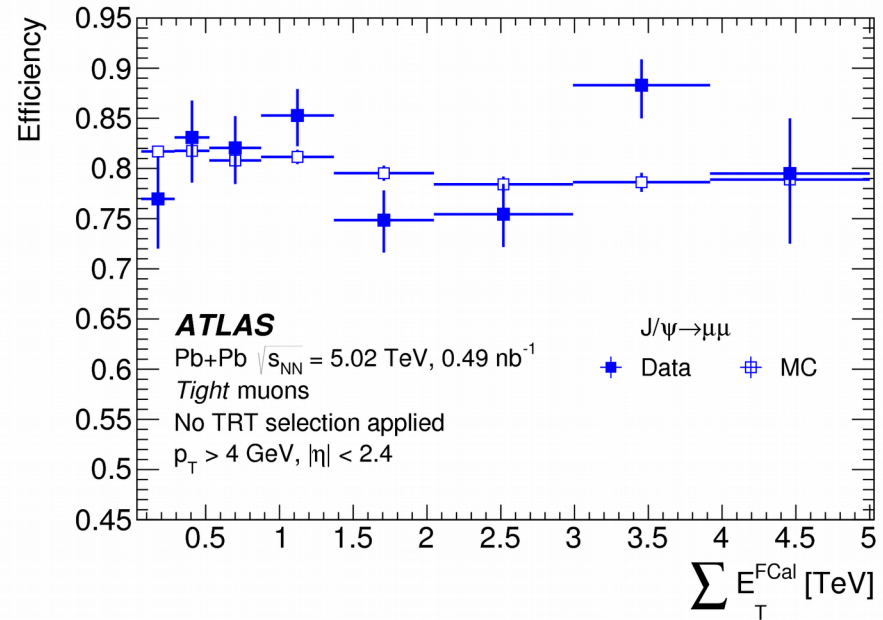
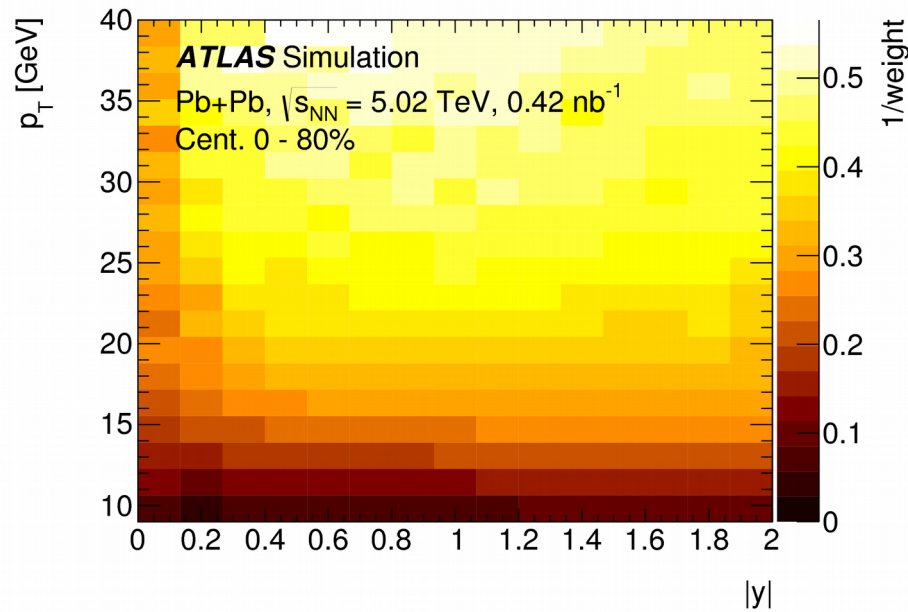
Not covered in this talk, but unmissable:

- Jet fragmentation functions at 5.02 TeV - 1805.05424
- Flow cumulants - 1807.02012
- J/ψ elliptic flow - 1807.05198
- R_{AA} and flow of HF muons - 1805.05220

<https://twiki.cern.ch/twiki/bin/view/AtlasPublic/HeavyIonsPublicResults>

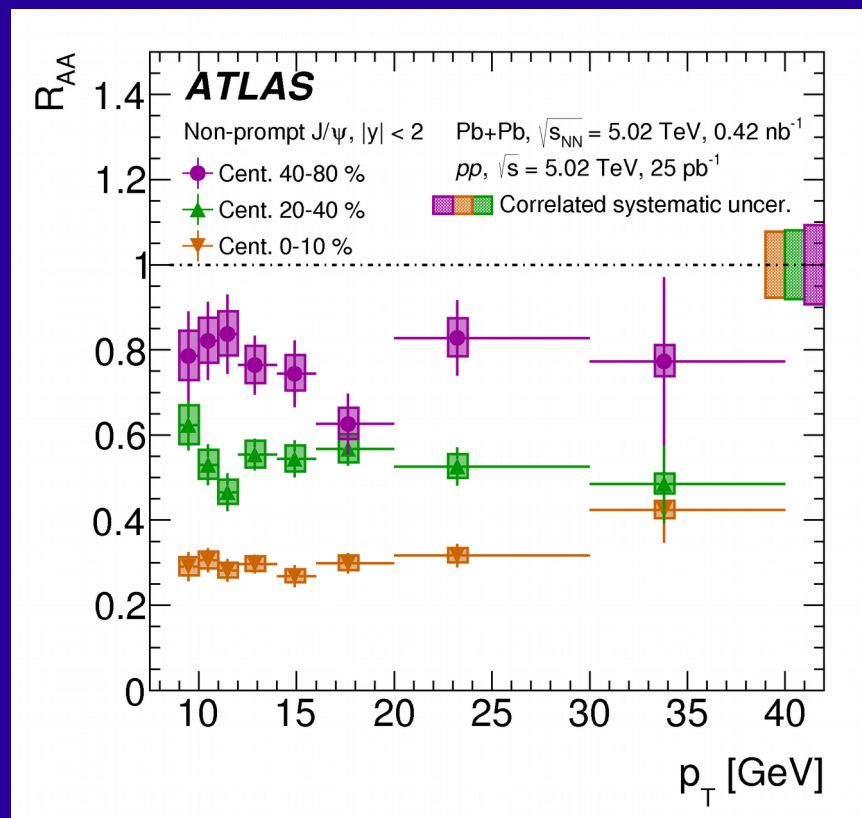
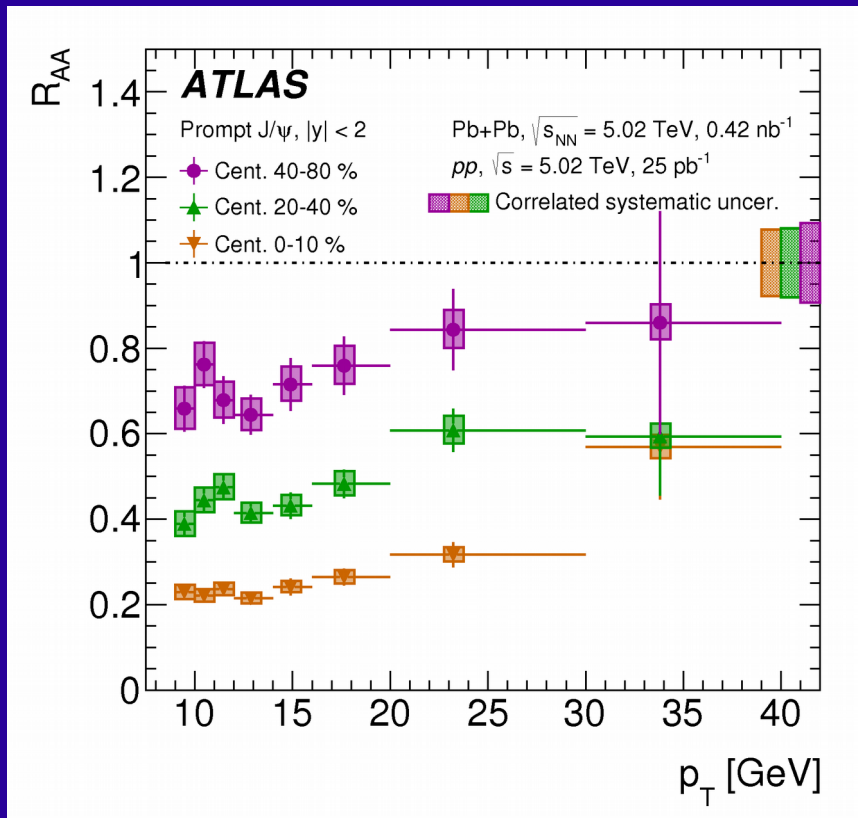
Backup

ATLAS Performance

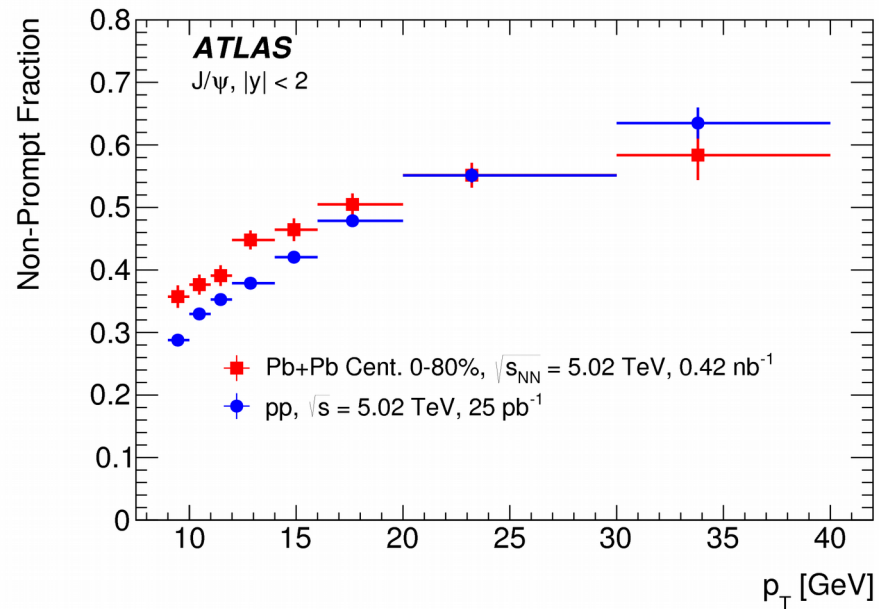
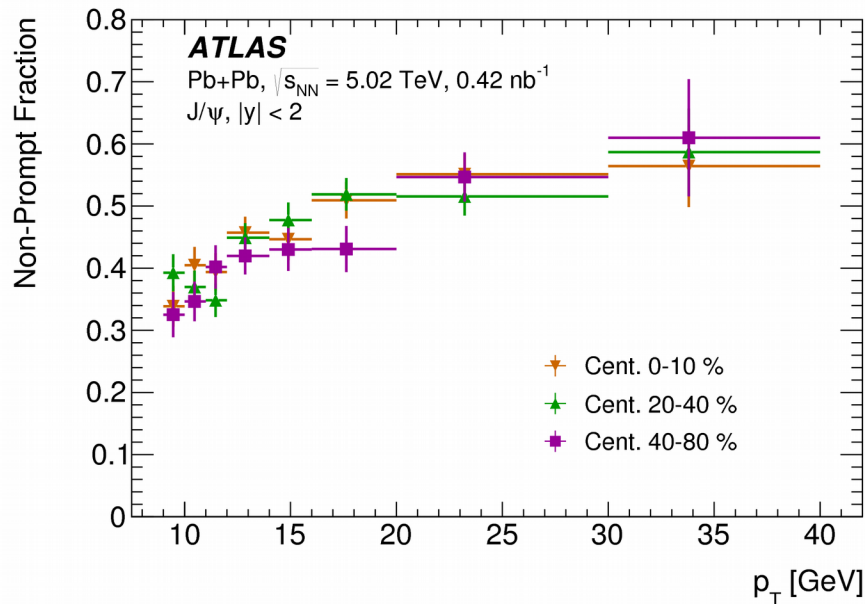


No dependence of the muon reconstruction efficiency on centrality.

J/ψ R_{AA} as a function of p_T



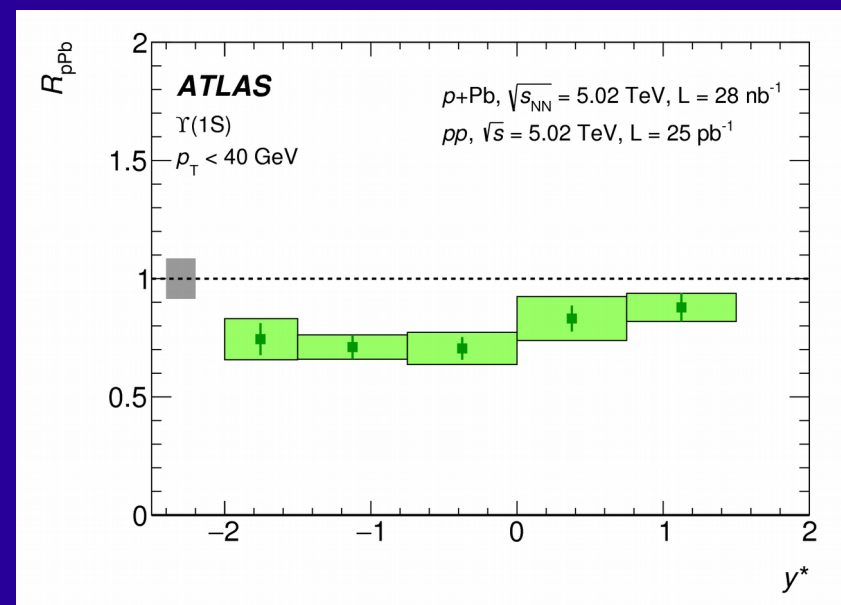
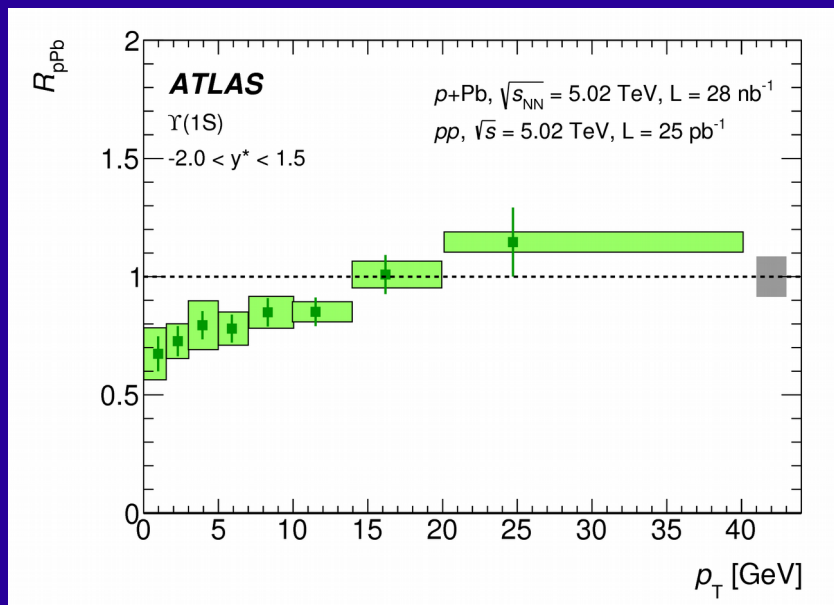
non-prompt fraction



- Nearly independent on centrality.
- Slight difference from pp.

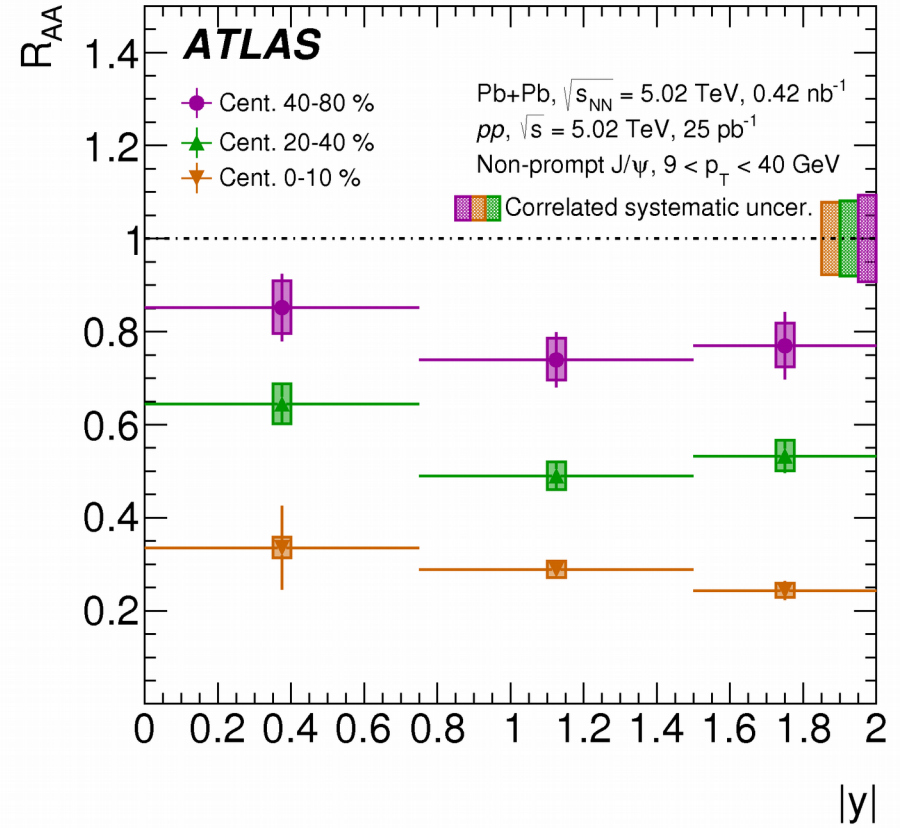
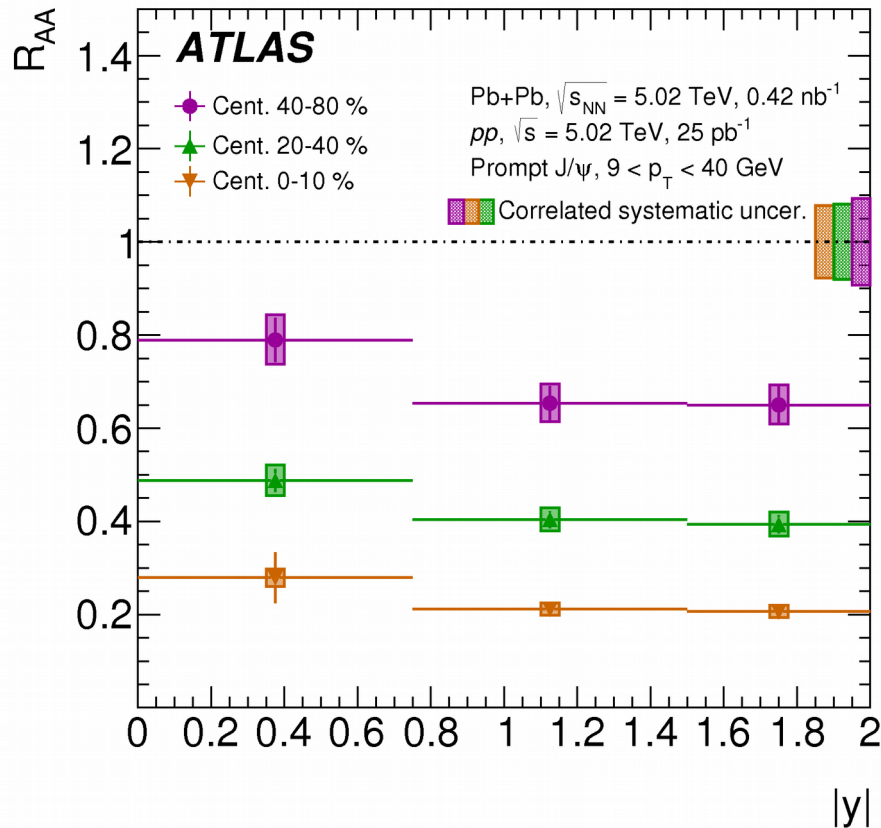
Upsilon R_{pPb}

arXiv1709.03089



J/ψ R_{AA} as a function of $|y|$ and centrality

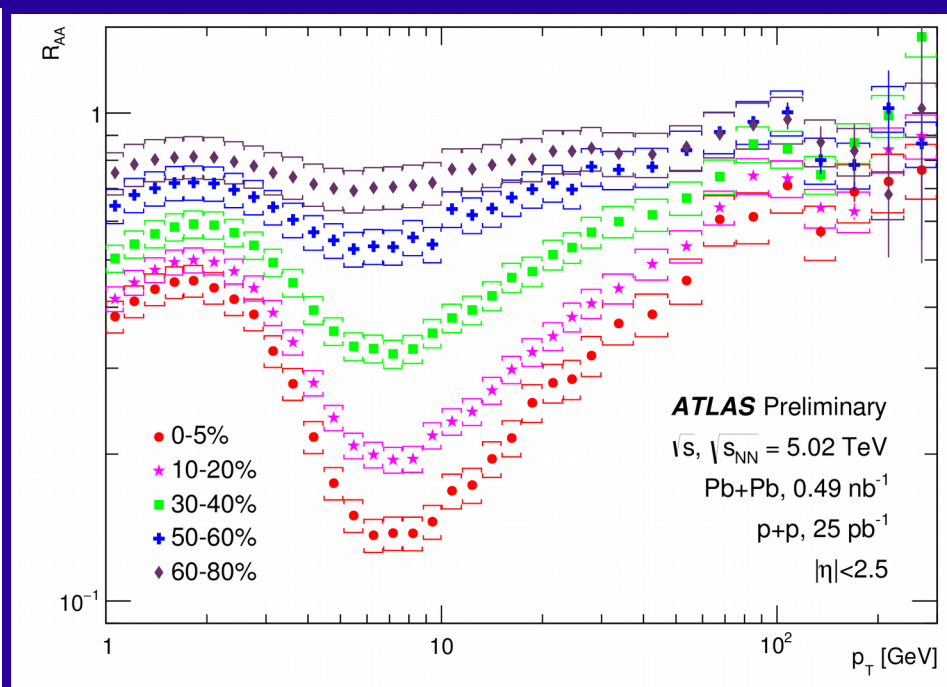
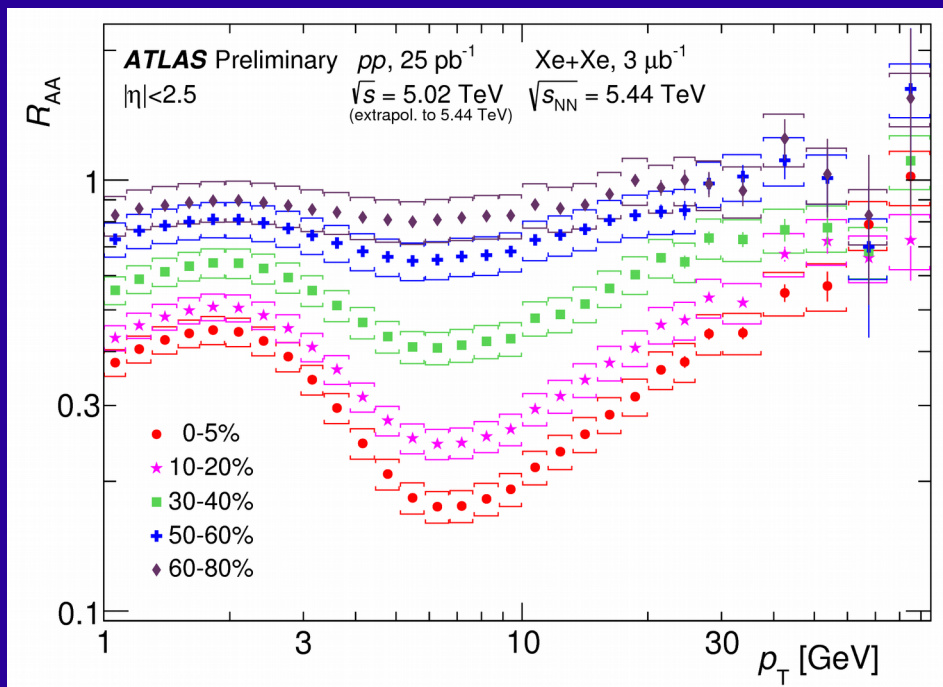
37

prompt**non-prompt**

Modest dependence on rapidity for both
prompt and non-prompt J/ψ.

Charged Hadron R_{AA} in Xe+Xe and Pb+Pb³⁸

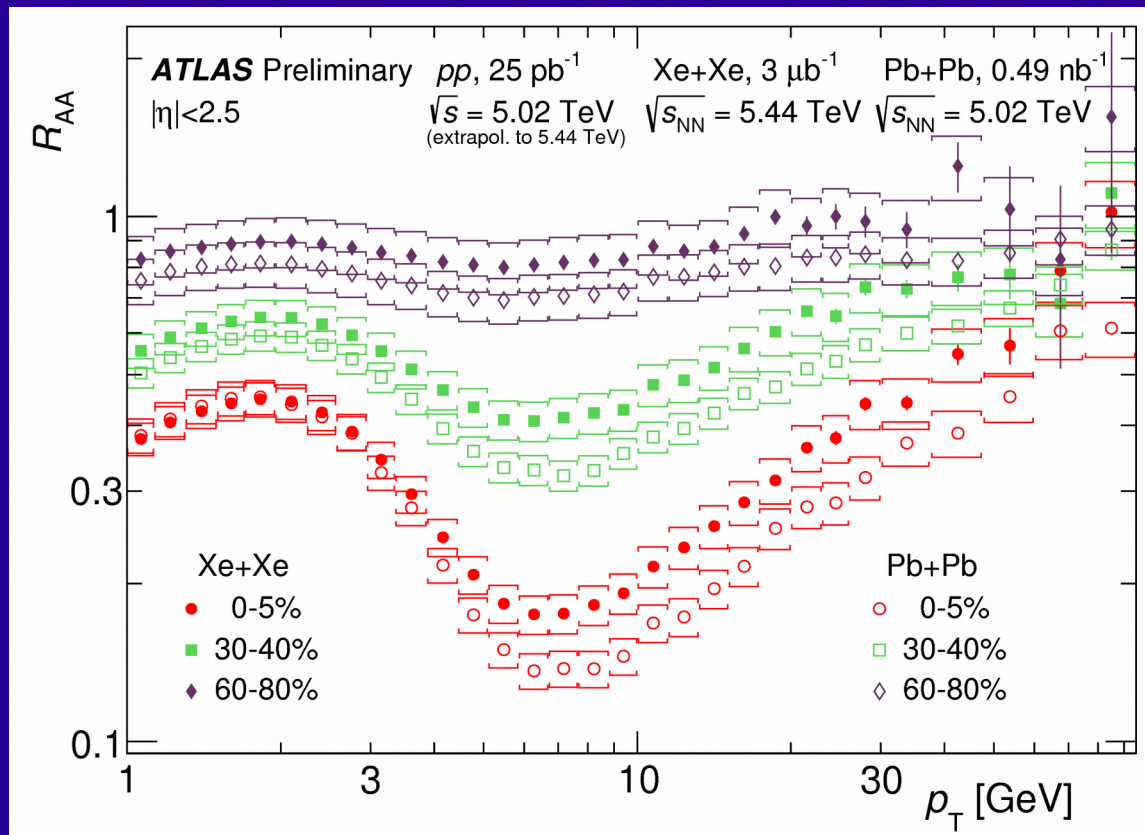
ATLAS-CONF-2018-007



- Note different x-axis
- Qualitatively similar

Charged Hadron R_{AA} in Xe+Xe and Pb+Pb³⁹

ATLAS-COEF-2018-007

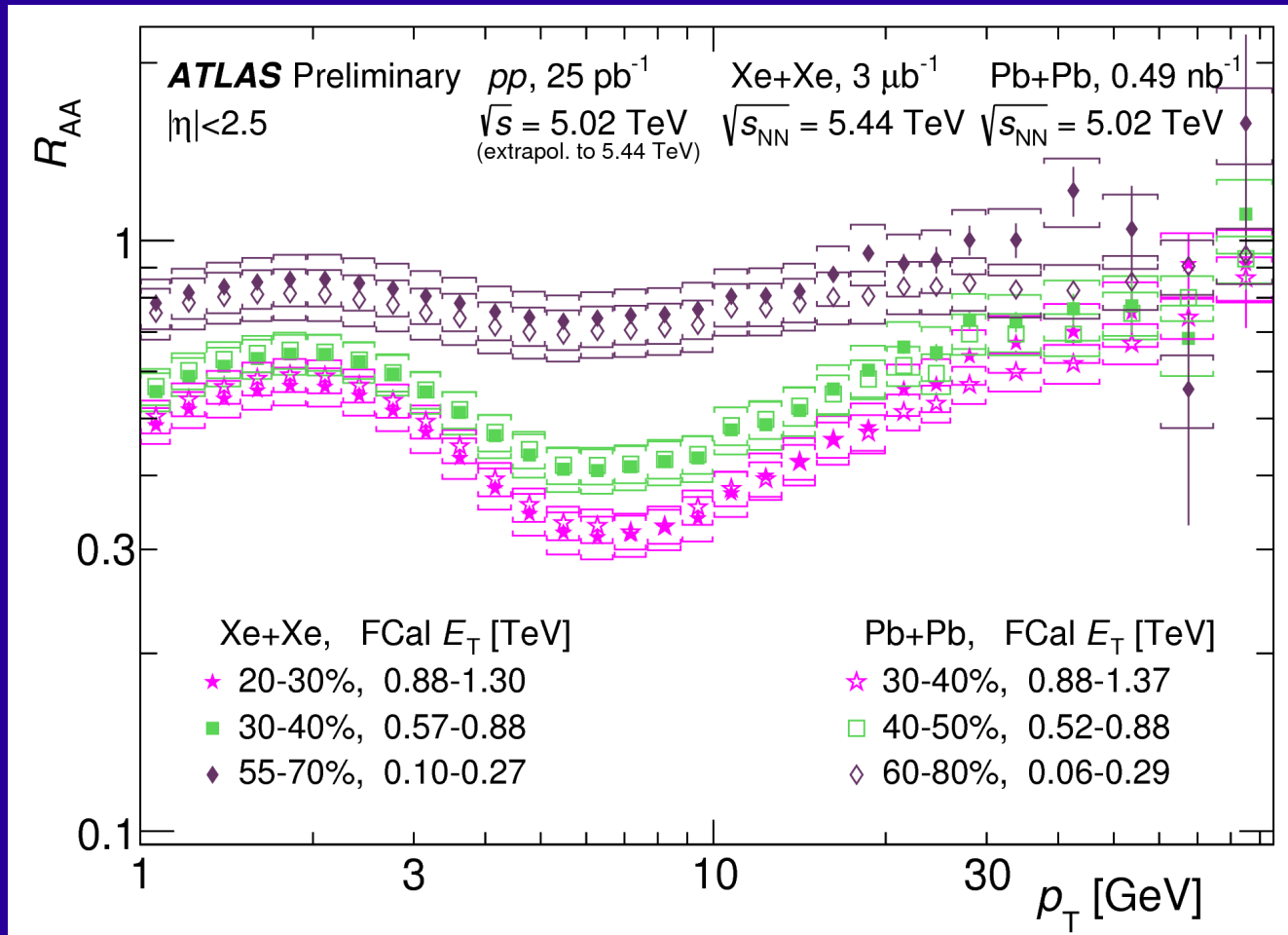


Same colours,
same centrality

- R_{AA} is very similar at low p_T in central collisions.
- Otherwise Xe+Xe is less suppressed than Pb+Pb.

Charged Hadron R_{AA} in Xe+Xe and Pb+Pb⁴⁰

ATLAS-COEF-2018-007

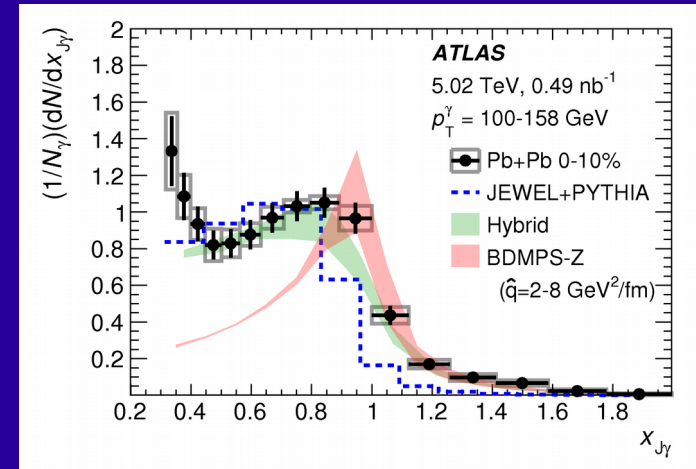
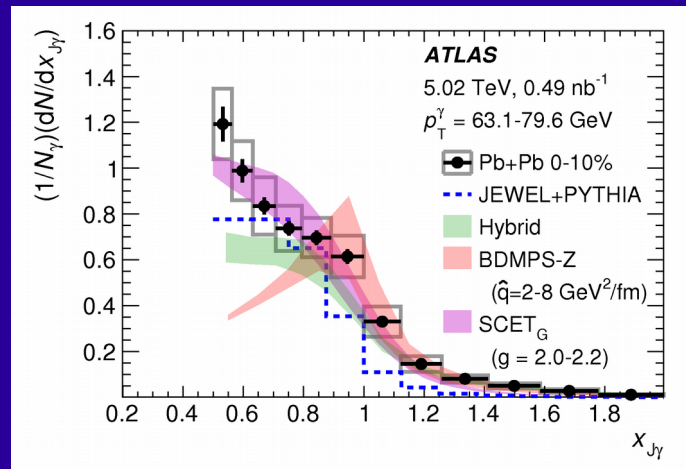
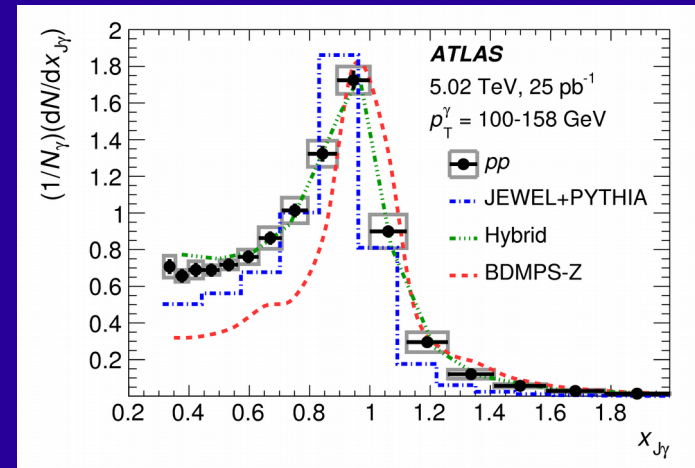
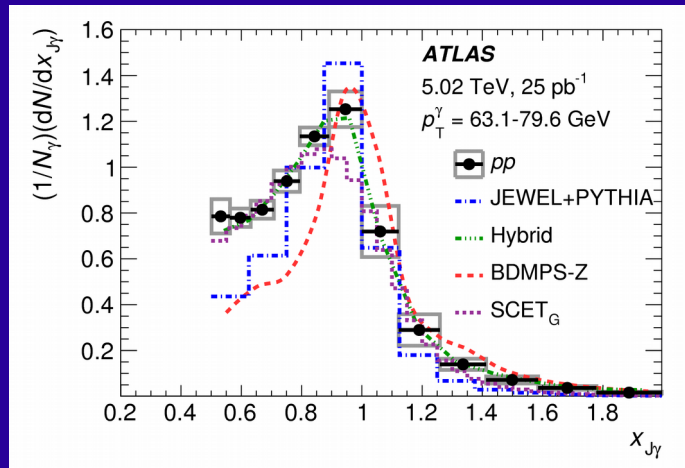


Same colours, same energy deposited in FCal

Electroweak probes: γ + jet p_T balance

10

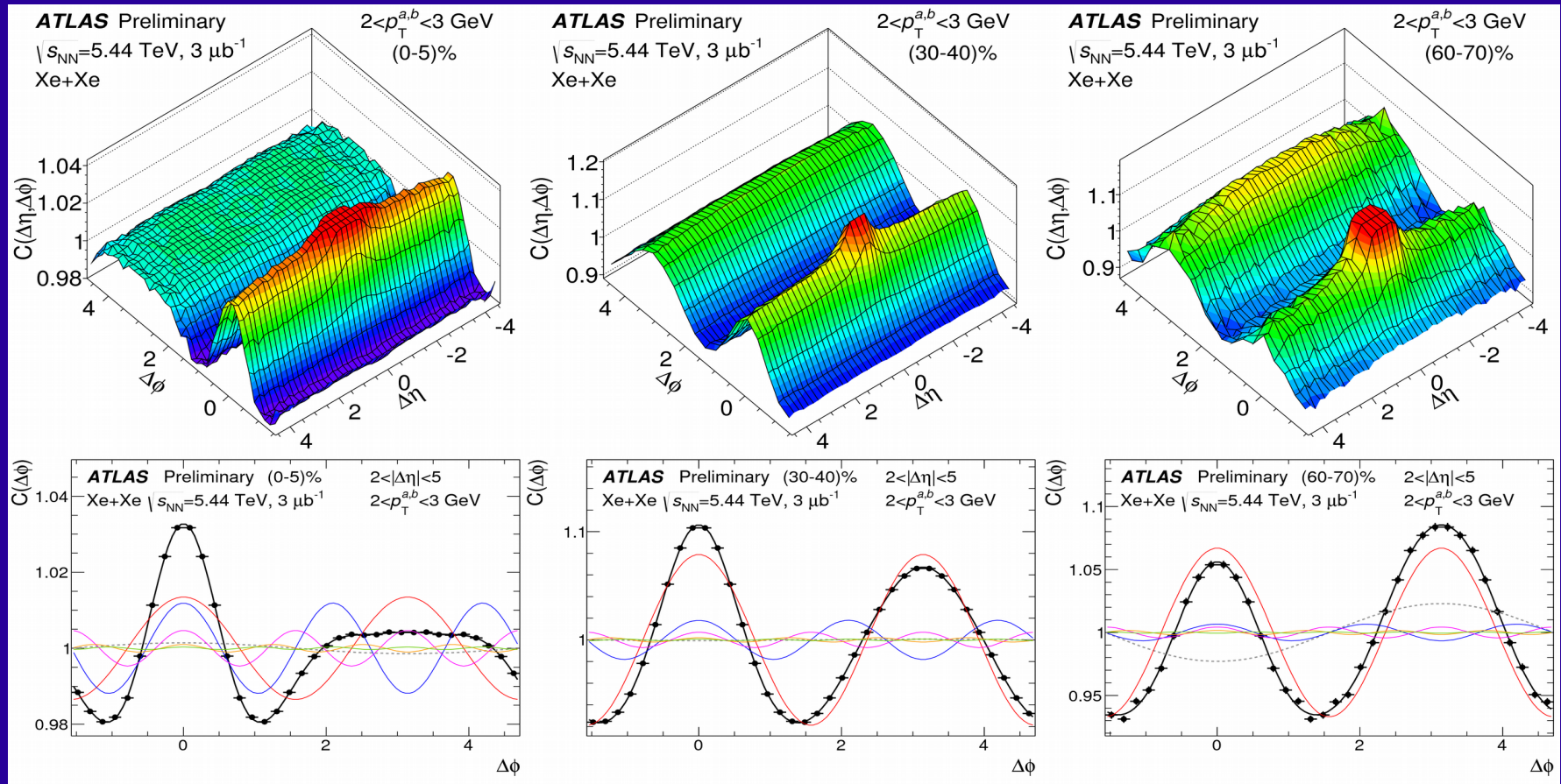
Phys. Lett. B 789 (2019) 167



Two-particle correlations in Xe+Xe collisions

ATLAS-CONF-2018-011

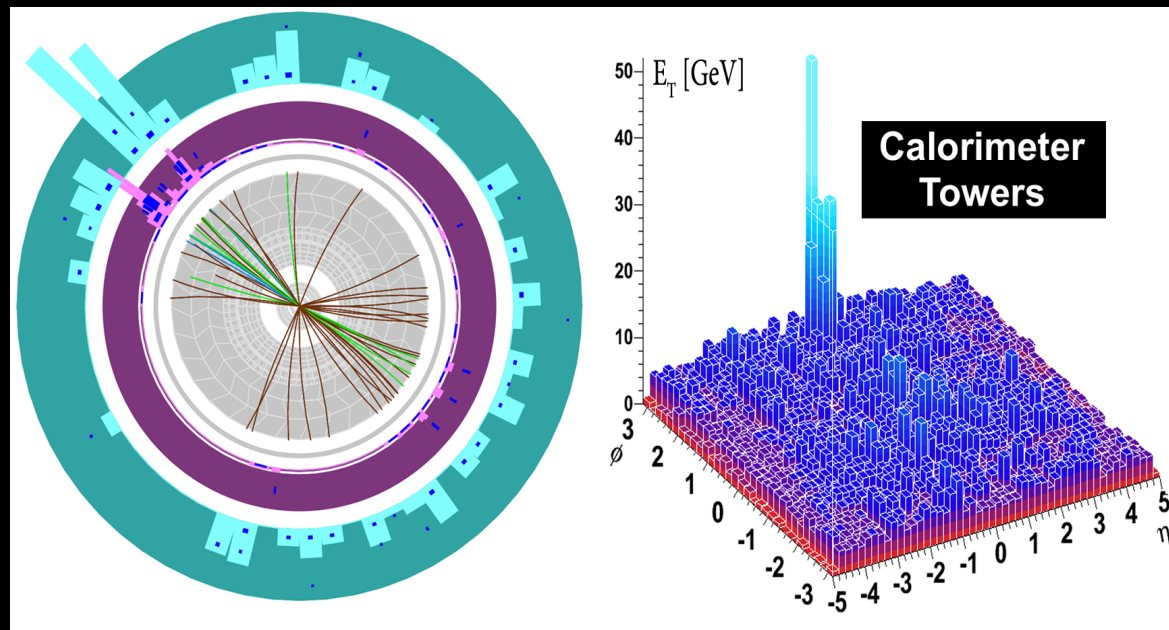
Flow harmonics, v_2 — v_5 , have been measured in Xe+Xe at 5.44 TeV using 2-PC



- Short-range ($\Delta\eta, \Delta\phi \sim 0, 0$) correlations in all centralities are due to non-flow processes.
- Long-range ($\Delta\eta$ large) correlations are the result of the global anisotropy of the event.

Jet Reconstruction in the Detector

- Jets are reconstructed by computational algorithms that group “towers” of energy deposited in the calorimeters.
- The Underlying Event (“background”) is estimated event-by-event, excluding the jet candidate.



Jet Reconstruction

- Underlying event estimated and subtracted for each longitudinal layer and for 100 slices of $\Delta\eta = 0.1$:

$$E_{T,subt}^{cell} = E_T^{cell} - \rho \times A^{cell}$$

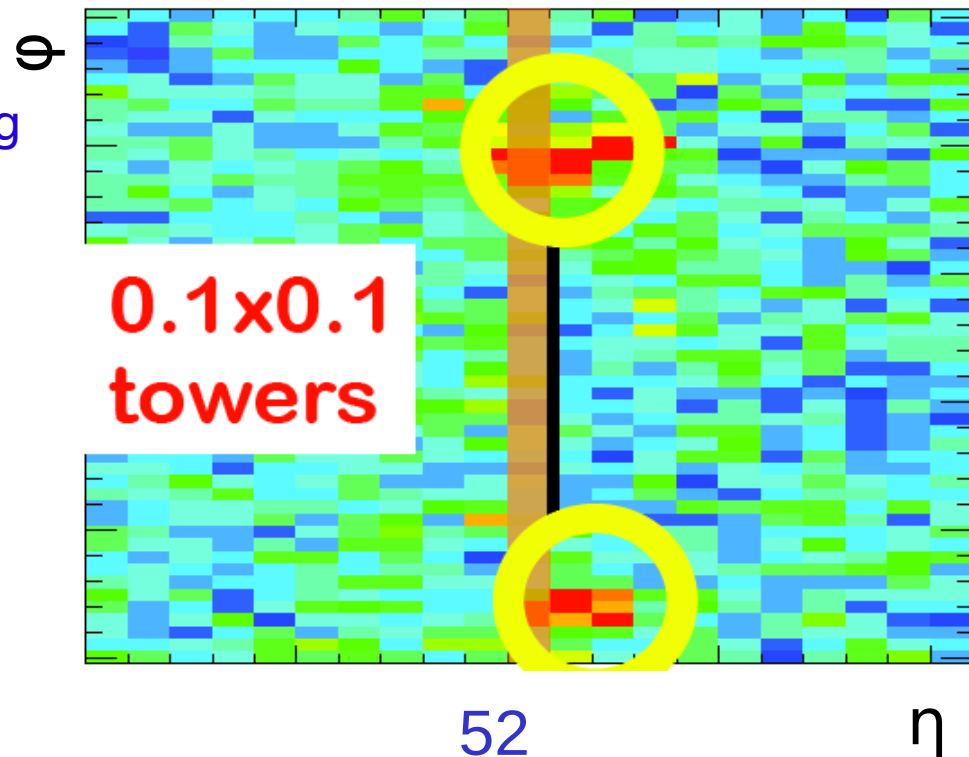
ρ is energy density estimated event-by-event from average over $0 < \phi < 2\pi$

- Two methods to avoid biasing ρ due to jets

- Sliding window exclusion
- Exclude cells in jets satisfying

$$D = E_{T,max}^{tower} / \langle E_T^{tower} \rangle > 5$$

- For $R = 0.4$, add an iteration step to ensure jets with $E_T > 50$ GeV are always excluded from ρ estimate
- Correct for underlying event v_2

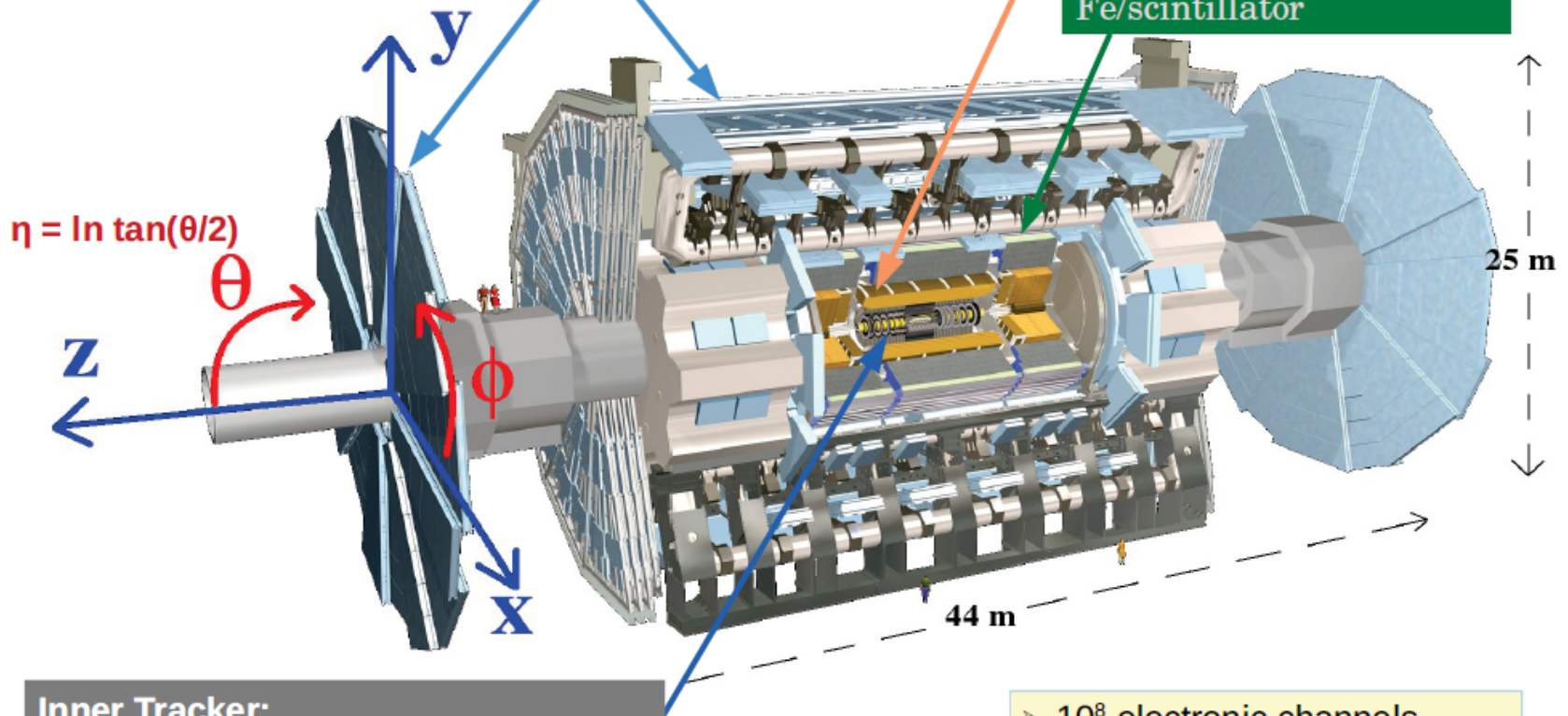


ATLAS

Muon Spectrometer:
Air-core toroids and gas-based muon chambers

EM calorimeter:
Pb-LAr Accordion

Hadronic calorimeter:
Fe/scintillator



Inner Tracker:
Si pixels/strips and straw detector

- > 10^8 electronic channels
- > 1,6 MB per event (64 TB/s)

Longitudinal flow decorrelations 7

Space-time evolution of the matter created is not boost-invariant in the longitudinal direction: $v_n(\eta_1) \neq v_n(\eta_2) \rightarrow$ FB asymmetry

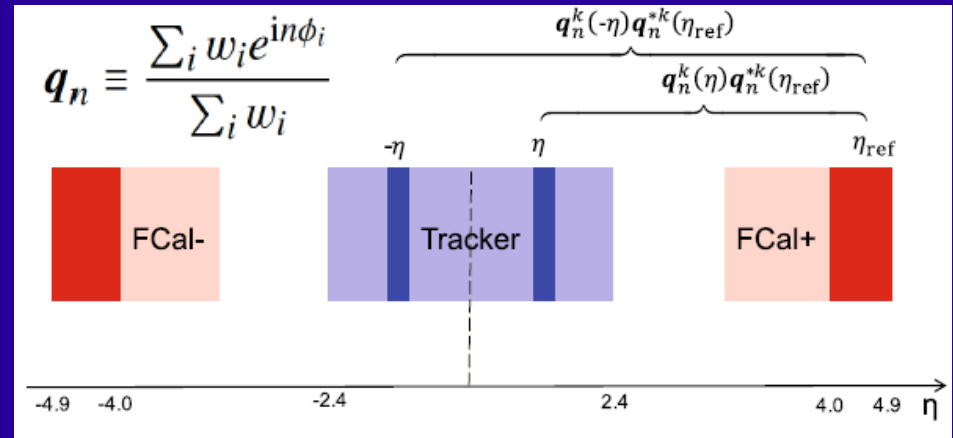
$\Phi_n(\eta_1) \neq \Phi_n(\eta_2) \rightarrow$ sensitivity to twists

Harmonic flow vectors measured with charged particles over $|\eta| < 2.5$:

$$\vec{v}_n(\eta) = v_n(\eta) e^{in\Phi_n(\eta)}$$

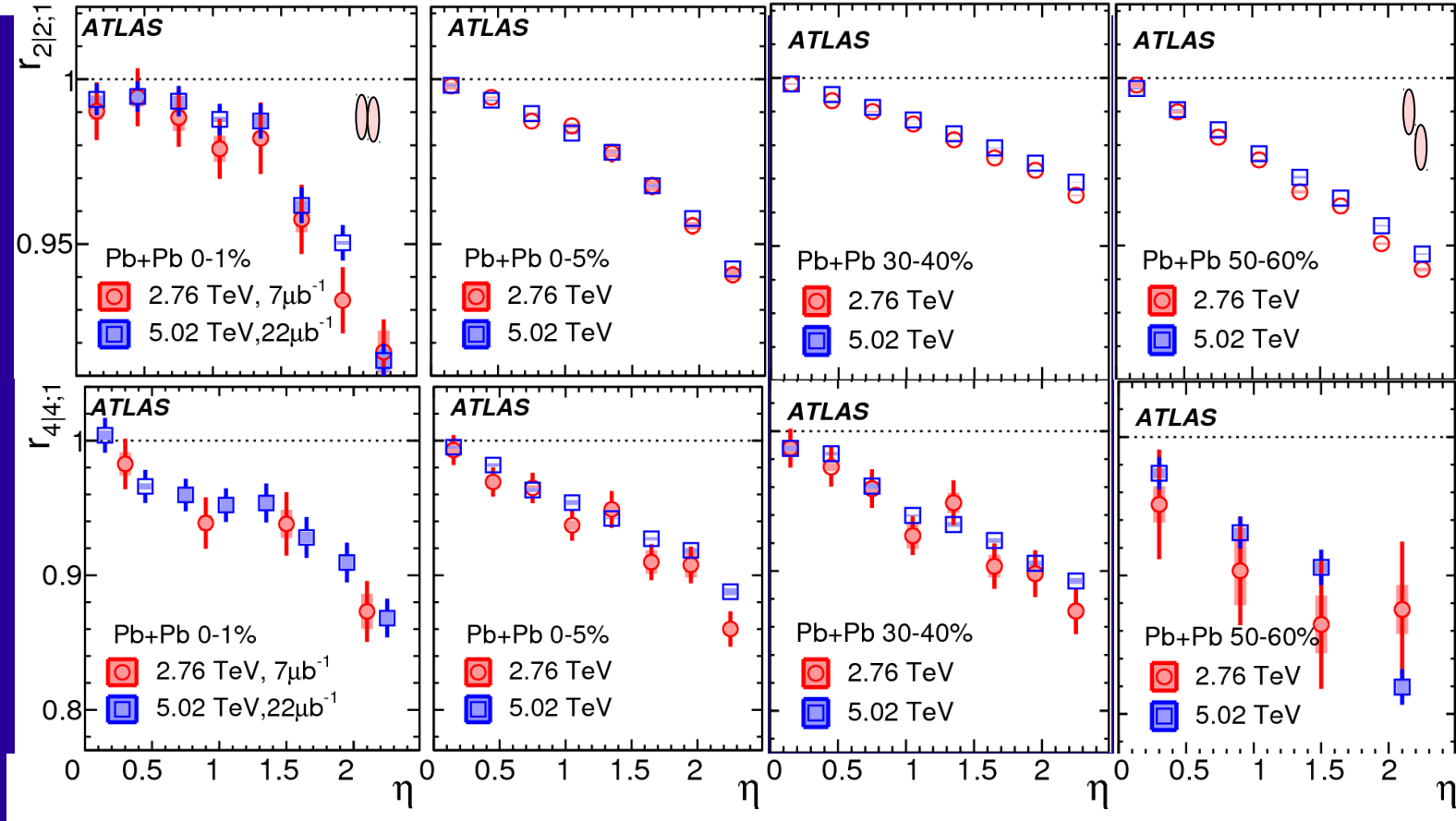
Decorrelations \rightarrow use $r_{n|n;k}$ between the k th-moment of the n th-order flow vectors in two different η intervals:

$$r_{n|n;k}(\eta) = \frac{\langle \mathbf{q}_n^k(-\eta) \mathbf{q}_n^{*k}(\eta_{\text{ref}}) \rangle}{\langle \mathbf{q}_n^k(\eta) \mathbf{q}_n^{*k}(\eta_{\text{ref}}) \rangle}$$



Longitudinal flow decorrelation in Pb+Pb collisions

Eur. Phys. J. C 76 (2018) 142



- $r_{n|n,k}$ shows a linear decrease with η_{ref} , except in the most central collisions.
- The decreasing trend of $r_{n|n,k}$ for $n \equiv 2-4$ indicates significant breakdown of the factorisation of two-particle flow harmonics.
- The decreasing trend is slightly stronger at 2.76 TeV (collision system less boosted).